

# Assessing climate change impacts on surface water availability using the WEAP model: A case study of the Buffalo river catchment, South Africa

N. Dlamini<sup>a,\*</sup>, A. Senzanje<sup>a</sup>, T. Mabhaudhi<sup>b,c</sup>

<sup>a</sup> Bioresources Engineering Programme, University of KwaZulu-Natal, P. Bag X01, Scottsville, Pietermaritzburg, South Africa

<sup>b</sup> Centre of Transformative Agricultural and Food Systems, University of KwaZulu-Natal, P. Bag X01, Scottsville, Pietermaritzburg, South Africa

<sup>c</sup> International Water Management Institute (IWMI-SA), South Africa, Pretoria, South Africa

## ARTICLE INFO

### Keywords:

Hydrological modelling  
Water balance  
Water-Energy-Food nexus  
Sustainability

## ABSTRACT

*Study region:* The Buffalo River (BR) catchment, KwaZulu-Natal, South Africa.

*Study focus:* Due to the vast majority of the BR catchment's water demands not being fully satisfied in recent years, studies investigating potential climate change impacts on the catchment's water supply availability are needed. The study's objective was to therefore assess climate change-induced surface water availability (SWA) variations in the BR catchment from 2020 to 2100. To achieve this, the hydrologic Water Evaluation and Planning model was forced with the catchment's physical and hydrological data, and projected climate data from an ensemble of GCMs under RCP4.5 and RCP8.5 scenarios from CMIP5.

*New hydrological insights for the region:* The study findings projected increased precipitation, especially in the far future (2070–2100) whereby mean annual precipitation increased by 5 % to 8286 Mm<sup>3</sup>/annum under the worst-case climate change scenario (RCP8.5). With evapotranspiration and water abstractions averaging 4500 Mm<sup>3</sup>/annum and 115 Mm<sup>3</sup>/annum, respectively, surface runoff and SWA increased by 8 % and 10 %, yielding averages of 3265 Mm<sup>3</sup>/annum and 287 Mm<sup>3</sup>/annum, respectively. Even with the increased SWA, unmet demands also increased by 113 % towards the end of the 21st century. As the study established that climate change might exacerbate the BR catchment's water supply system's insufficiency to meet growing demands, such findings present an opportunity for the integrated Water-Energy-Food nexus approach to be further utilised for formulating sustainable water management strategies.

## 1. Introduction

Climate change (CC) might perpetuate increased water demands and water scarcity caused by population growth and economic development through changes in rainfall magnitude and variability (DEA, 2012; Erler et al., 2019; Exposito et al., 2020). The gap that exists in many regions globally between water demand and supply capacity increases competition among various users (Exposito et al., 2020). Investigating CC impacts on water availability is thus crucial, especially in matters pertaining to the sustainable development of CC adaptation and resilience strategies (Erler et al., 2019).

The Water-Energy-Food (WEF) nexus is an approach for better understanding and methodically analysing the interactions between

\* Corresponding author.

E-mail address: [nosiphodlamini27@gmail.com](mailto:nosphodlamini27@gmail.com) (N. Dlamini).

the natural environment and human activities to achieve more coordinated management and use of natural resources across sectors and scales (McNamara et al., 2018). Building on the Integrated Water Resources Management (IWRM) approach, which is water-centric, the goal of the WEF nexus is to approach resource management holistically by using a poly-centric philosophy (Mabhaudhi et al., 2018).

WEF nexus assessments can be carried out using conceptual visualisation tools (CVT) or quantitative analytical tools (QAT), all of which constitute modelling tools. Frequently, modelling tools employ monthly time series data for parameters (e.g. climate, water and crop yields, agricultural areas and energy generation) to simulate determined target values based on various inputs (McNamara et al., 2018). The simple manner in which models represent and simulate processes serves their advantage (Parra et al., 2018). They can be used to assess a system’s sensitive components and simulate future scenarios for decision support in planning (McNamara et al., 2018). For water and basin management, the use of water balance models has recently increased, especially in CC impact studies and for the simulation of different environmental processes (Parra et al., 2018).

The Water Evaluation and Planning (WEAP) system model, developed by the Stockholm Environment Institute (SEI), is an integrated approach used to simulate both natural and engineered hydrological components of a water system’s demands and supplies (Sieber, 2015). The WEAP model is classified as an IWRM tool due to its water-centric nature (Tena et al., 2019). However, since WEAP

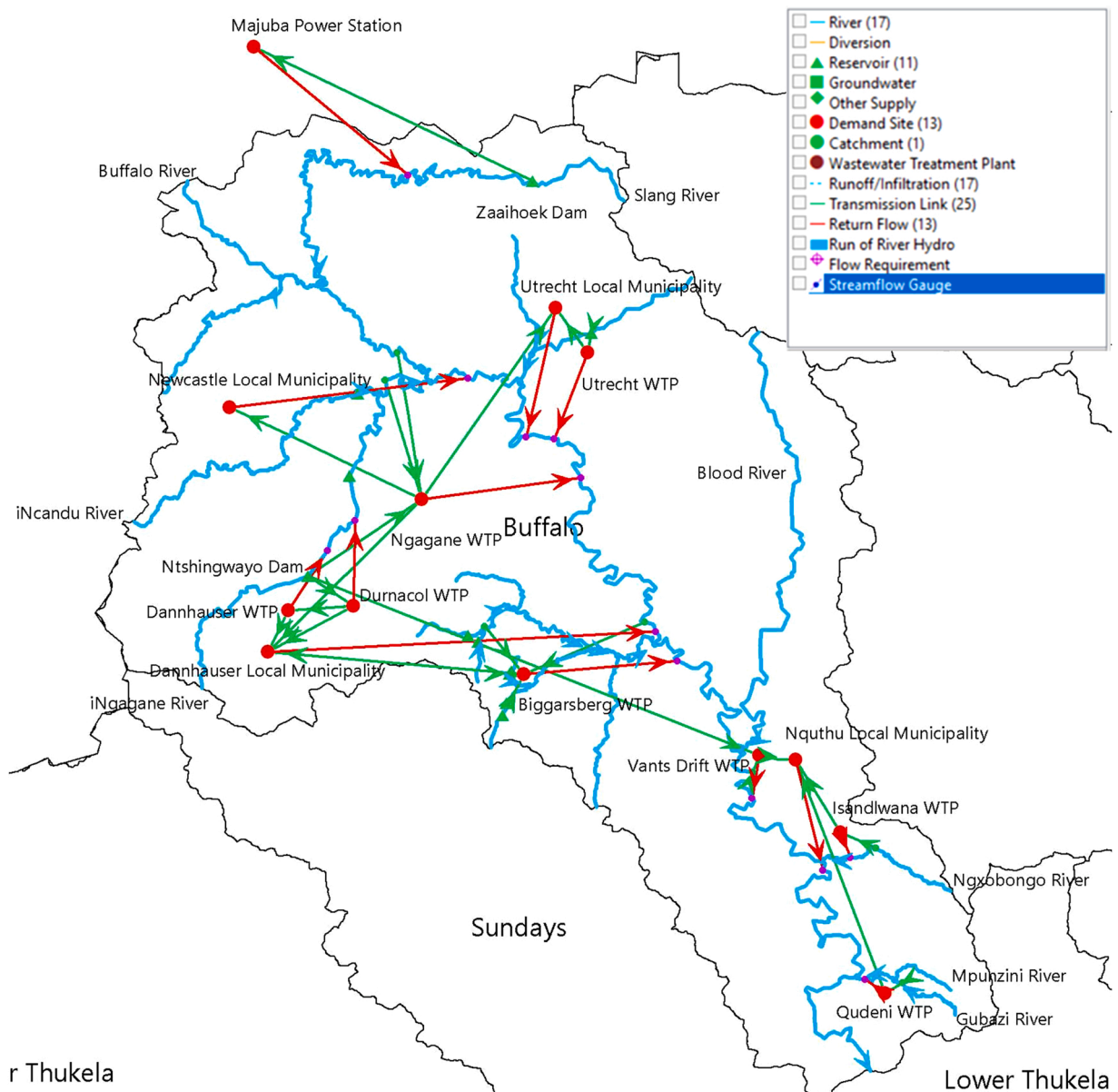


Fig. 1. General layout of the Buffalo River catchment, KwaZulu-Natal, South Africa.

is designed to interact with other models, it is used as a WEF nexus QAT through integration with food- and energy-centric models. This gave rise to the Climate, Land-use, Energy and Water strategies (CLEWs) WEF nexus modelling framework (Howells et al., 2013), used internationally and within Africa.

To introduce integrated land and water management, the Government of Rwanda, for example, is currently developing plans for four selected demonstration catchments using the WEAP modelling tool (Droogers et al., 2017). The island of Mauritius also utilised the WEAP model for simulating river systems in 60 catchments to assess the implications of local, municipal and agricultural water requirements on national water supply schemes (Welsch et al., 2014).

Several water availability and management studies were performed in South Africa using the WEAP model. For example, Levite et al. (2003) evaluated the usefulness of WEAP in assessing water demand management scenarios in the Steelpoort sub-catchment of the Olifants River through the analyses of simulated catchments' met and unmet demands. Arranz and McCartney (2007) used WEAP to assess the impacts of likely future water use on the water resources of the Olifants catchment. Haji (2011) investigated the effects of future CC on meeting the water demands of different consumers in the Upper Vaal River Basin using the WEAP model. These studies concluded that WEAP is useful for water resources assessment in South African catchments and for a holistic view of an entire river basin.

The Buffalo River (BR) catchment is a sub-catchment of the Thukela Water Management Area, whose water source is in the Drakensberg region. The BR catchment is characterised as a relatively high runoff sub-catchment (Dlamini and Schulze, 2006) that supplies water to numerous sectors, including irrigation, power generation, domestic, mining and bulk industries (StatsSA, 2010). There have been severe droughts in past years, especially during 2015–2016, which consequently affected the livelihoods and socio-economic activities of local and surrounding communities, as well as the capability of the catchment's water supply system to meet its water demands (uMgeni, 2020). Thus, an integrated surface water availability assessments is essential in such cases for the effective and responsible management of water resources (Tena et al., 2019).

Previous studies that investigated the long-term changes of the water supply-demand relationship within the BR catchment primarily focused on whether current water supplies are sufficient to meet projected population demand, rather than how climate change may influence and change the quantity of water stored and made available to users (DWAf, 2003; DWA, 2011; uMgeni, 2016, 2020). To our knowledge, a detailed climate change and water resources analysis has not been undertaken for the BR catchment (uMgeni, 2020). Therefore, the objective of this study was to assess the impacts of CC on surface water availability in the BR catchment. It is difficult to predict and quantify the exact available surface water and water balance. Hence, a scenario analysis was chosen as the most appropriate approach to meet the objective using the WEAP modelling tool.

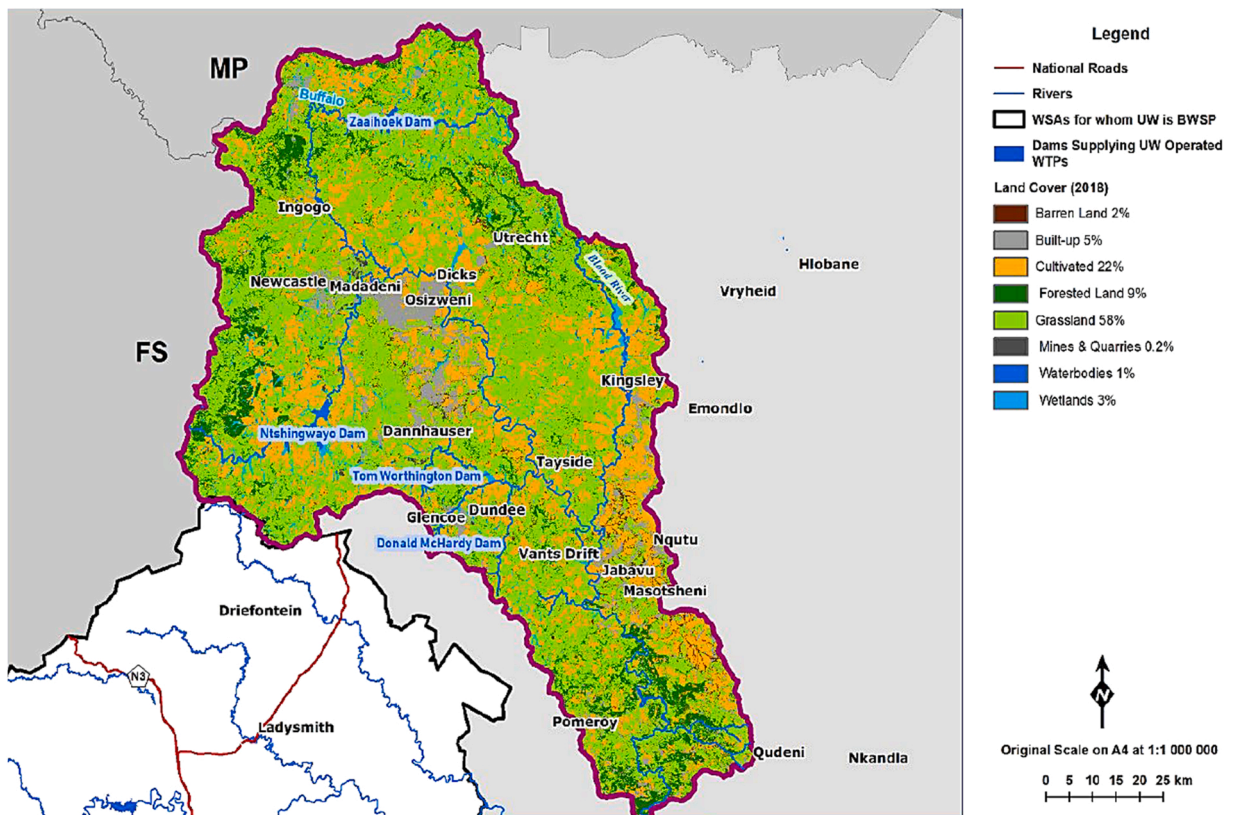


Fig. 2. Land-use in the Buffalo River catchment (uMgeni, 2020).

## 2. Materials and methods

### 2.1. Study site description

The BR catchment, covering an estimated area of 9 803 km<sup>2</sup>, has minimum latitude and maximum longitude values of 28° 42' 59" S and 30° 38' 30" E, respectively (uMgeni, 2020). The catchment is situated in a warm and humid region that receives most of its annual rainfall during summer. As per Fig. 1, the BR is the main northern tributary of the uThukela River. It flows approximately 339 km south-easterly from the eastern escarpment (Newcastle area) through the Amajuba and uMzinyathi District Municipalities, then confluences with the uThukela River in the Msinga Local Municipality (Dlamini and Mostert, 2019; uMgeni, 2020).

The predominant land cover in the BR catchment is grassland (58 %), followed by cultivated land (22 %), as seen in Fig. 2 (uMgeni, 2020). Grassland is mostly utilised for the grazing of livestock (INR, 2019). Commercial-scale production of maize, soybean and wheat dominates the upper catchment region, with irrigated production mainly taking place in the fertile region of the western Newcastle Local Municipality (StatsSA, 2017; LGCCP, 2018). Commercial and subsistence farming under rainfed conditions is more prominent in the BR catchment's middle and lower southern regions (StatsSA, 2017).

### 2.2. Hydrological characteristics

The hydrological characteristics of the BR catchment are summarised in Table 1. The upper tertiary catchment V31, where the Slang, iNcandu and iNgagane rivers are located, generates the largest mean annual runoff of 119 mm (DWS, 2015; uMgeni, 2020). This can be mainly attributed to the high rainfall and steeper gradient of the Drakensberg Mountains regions (uMgeni, 2020). However, mean annual runoff trends have been noted to decrease as the BR traverses to the middle (V32) and lower (V33) regions, yielding 73 and 64 mm/annum, respectively (DWS, 2015; uMgeni, 2020).

### 2.3. Surface water infrastructure

The total supply capacity of the BR catchment's existing surface water infrastructure is approximately 405 Mm<sup>3</sup>, providing a hydrological yield of 136.9 Mm<sup>3</sup>/annum (unspecified assurance level). The Ntshingwayo Dam contributes significantly to the water supply, with a full supply capacity of 211 Mm<sup>3</sup> and yield of 59 Mm<sup>3</sup>/annum, as well as the Zaaiohoek Dam, with a full supply capacity of 185 Mm<sup>3</sup> and yield of 54 Mm<sup>3</sup>/annum (uMgeni, 2020). The BR catchment's water supply system (BR system) also includes eight water treatment plants (WTP) which, as listed in Table A.1, extract water from supply sources and distribute it to their designated supply areas. Other WTPs within the BR system, such as the Charlestown WTP, are primarily supplied by groundwater sources, and distribute approximately 440 kl/day to their respective water demand sites (uMgeni, 2020). Due to the lack of data availability related to the location and distribution of these groundwater resources, the aforementioned WTPs were not included in this study.

### 2.4. WEAP model description

The WEAP model is an "innovative, integrated modelling software that offers a detailed, dynamic and user-friendly framework for establishing water balances, scenario generation, planning and policy analysis" (Ayele, 2016; Tena et al., 2019). The model was developed for integrated water resources planning (Tena et al., 2019) and can be applied to municipal and agricultural systems, and to a single catchment or a complex transboundary river basin system (Ayele, 2016). The WEAP model simulates a wide range of natural and engineered components of the aforementioned systems, from precipitation to streamflow, reservoirs, groundwater discharge and water demand and supply (Agarwal et al., 2018).

#### 2.4.1. WEAP model water balance computation

The WEAP model was used to simulate the water balance components in Eq. 1 (Sieber, 2015) using climate, physical and hydrological inputs from the BR catchment, and the modelling process used is visualised in Fig. 3. Actual evapotranspiration included evaporation losses from vegetation and open water bodies. Streamflow comprised of surface runoff only, i.e., no groundwater contributions. Hence, the impact of groundwater recharge on reservoir storage was assumed negligible. However, it is important to note that there are five hydrogeological units comprising one primary- and four secondary-type aquifers within the BR catchment. They exhibit moderate potential to provide mean yields of 0.9–2.7 l per second (l/s) via boreholes of 30–60 m deep (uMgeni, 2020). Thus, various water supply schemes within the BR catchment rely solely on groundwater supply from boreholes.

**Table 1**  
Buffalo River catchment hydrological characteristics (DWS, 2015).

Tertiary catchment	Area (km <sup>2</sup> )	Annual average		
		Evaporation (mm)	Rainfall (mm)	Natural Runoff (mm)
V31	3 948	1 435	851	119.0
V32	4 018	1 491	778	72.5
V33	1 837	1 477	747	64.2
Total	9 803	1 465.8	801.6	89.7

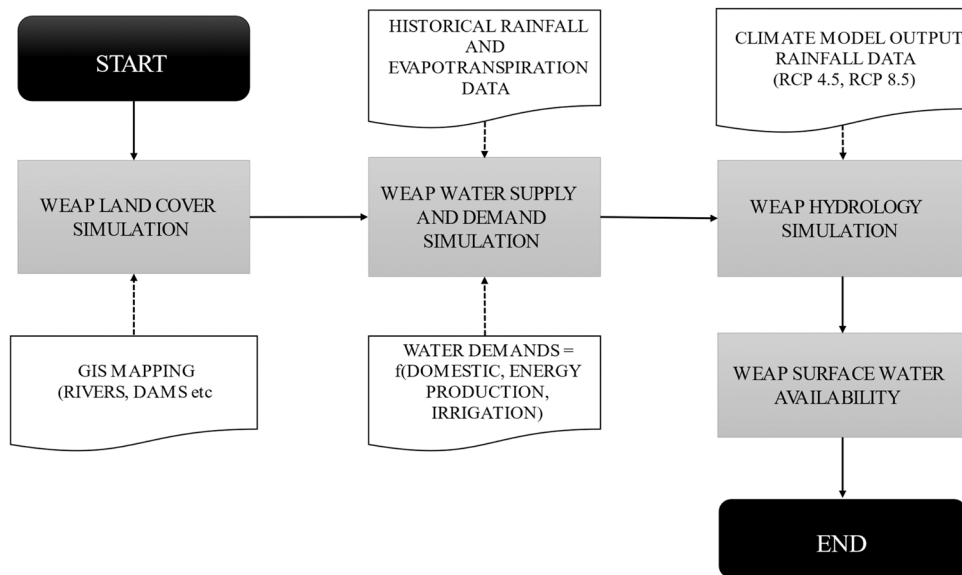


Fig. 3. Hydrological modelling process steps and the respective data requirements using the WEAP model.

$$P + E_x = ET_A + Q + W_A \pm \Delta S \quad (1)$$

where  $P$  = precipitation ( $\text{Mm}^3/\text{annum}$ ),  $E_x$  = external flows ( $\text{Mm}^3/\text{annum}$ ),  $ET_A$  = actual evapotranspiration ( $\text{Mm}^3/\text{annum}$ ),  $Q$  = streamflow @Buffalo River outlet ( $\text{Mm}^3/\text{annum}$ ),  $W_A$  = abstractions ( $\text{Mm}^3/\text{annum}$ ),  $\Delta S$  = change in reservoir storage ( $\text{Mm}^3/\text{annum}$ ).

There are five methods which WEAP can be used for water resources simulation: “(a) the Rainfall-Runoff and (b) Irrigation Demands Only versions of the Simplified Coefficient Approach, (c) the Soil Moisture Method, (d) the MABIA Method, and (e) the Plant Growth Model” (Sieber, 2015). The Rainfall-Runoff Simplified Coefficient Method was chosen due to the availability of data required by this approach. The Rainfall-Runoff method is similar to the Irrigation Demands Only method as they both use crop coefficients to compute potential evapotranspiration in the catchment. For the Rainfall-Runoff method, the remainder of rainfall not consumed by evapotranspiration is simulated as runoff to a river or can be proportioned among runoff to a river and flow to groundwater via runoff/infiltration links. It does not, however, track soil moisture changes (Sieber, 2015). The concept of water balance is based on mass conservation principles in a closed system (Sieber, 2015) and includes all water inflows and outflows in a catchment area (Tena et al., 2019).

#### 2.4.2. WEAP model scenario computation

A scenario is a plausible depiction of how the future may unfold based on a detailed and scientifically sound set of assumptions regarding key interconnections and driving factors (Arranz and McCartney, 2007). As it is impossible to forecast exactly how water demands and other variables affecting water supplies could change in the future, scenarios were employed in this study.

Initially, a Current Account of the BR catchment was created in the WEAP model. The Current Accounts represents the basic definition of the water system as it currently exists by providing a snapshot of actual water demands, resources and supplies for the system using historical data; it forms the foundation of all scenarios (Sieber, 2015). The Representative Concentration Pathways (RCPs), which are scenarios developed for the climate modelling community as a basis for near- and long-term modelling experiments (Vuuren et al., 2011), are named according to radiative forcing target levels for 2100, as per Table A.2. This study used the following three scenarios to evaluate CC impacts on surface water availability in the BR catchment, which are further elaborated on later (Section 2.5.3):

- The Baseline Scenario which reflects historical climate conditions and utilised for comparison purposes against RCP scenarios.
- The RCP4.5 Scenario which is a “stabilisation scenario that assumes climate policies are invoked to limit emissions and radiative forcing” (Thompson et al., 2011). Carbon emissions peak at mid-century at around 50% higher than the historical levels (Wayne, 2013).
- The RCP8.5 Scenario is a high emission scenario based on no policy-driven mitigation (Vuuren et al., 2011). “Emissions continue to increase rapidly through the early and mid-parts of the century.” Carbon dioxide concentration accelerates and reaches 1370 ppm by 2100 (Vuuren et al., 2011).

## 2.5. WEAP model input data

### 2.5.1. Buffalo river catchment schematic in WEAP

Using GIS-based vector data, a schematic of the BR catchment was created in the WEAP model (Fig. 1). The vector layers included: (a) KwaZulu-Natal (KZN) secondary drainage regions, (b) KZN district municipalities, (c) river network of the Amajuba and uMzinyathi district municipalities, and (d) dams within the Amajuba and uMzinyathi district municipalities. All vector layers were obtained from DWS (2016), and their attribute data were further sorted using ESRI's ArcGIS software (Version 10.6.0.8321, released on 17 July 2018).

For the purpose of computing the rates and quantities of water recharge and abstraction, thirteen demand nodes were created for the BR system's demand analysis. Every demand node corresponds to a particular group of water consumers: four represent the municipal demand (domestic and irrigation water demand), eight represent WTPs, and one represents the energy demands. All water demand nodes depend on surface water resources only. The WEAP model was run at the monthly time step, with the hydrological year starting in October and ending in September.

### 2.5.2. Historical climate data

The input precipitation data used in WEAP to simulate historical and current catchment conditions were obtained from the Climate Hazards Group infra-red Precipitation with Station dataset (CHIRPS; Funk et al., 2015). The CHIRPS dataset "builds on previous approaches to 'smart' interpolation and high-resolution techniques, where precipitation estimates are based on infra-red Cold Cloud Duration (CCD) observations" (Funk et al., 2015). The algorithm uses satellite information to represent sparsely gauged locations and provides daily, pentadal, and monthly rainfall estimates from 1981 to the near present at a 0.05° spatial resolution.

Since the projections timeframe for this study spans from 01/01/2020–31/12/2099, data for a 30-year baseline period (WMO, 2021) was acquired for the entire boundary of the BR catchment from 01/01/1990–31/12/2019 using 0.05° pixels of the CHIRPS gridded data. To ensure that the CHIRPS dataset represented the catchment's climate conditions, it was bias-corrected using the linear scaling (LS) method, as demonstrated in Eq. 2. The LS bias correction method was selected as it preserves the mean signal of the observed variable and yields very good hydrological performance when applied under a monthly approach (Ghimire et al., 2018). The scaling factor was derived using the catchment's observed MAP of 802 mm obtained from uMgeni (2020), with the CHIRPS MAP of 722.03 mm. (Gudmundsson et al., 2012)

$$P_{corr} = P_{raw} \times CF \quad (2)$$

where  $P_{corr}$  = bias corrected precipitation (mm).

$P_{raw}$  = raw precipitation data (mm)

$$CF = \text{scaling factor} = \frac{MAP_{observeddata}}{MAP_{rawdata}}$$

The resulting historical annual precipitation values increased over time, with the lowest values of 645, 584, and 574 mm noted in the years 1992, 2003 and 2015, respectively. This coincides with the findings by Dube and Jury (2003) and Ndlovu and Demlie (2020), which highlighted the droughts experienced in the KZN province during these years. An extreme peak in precipitation was modelled for the year 1995, which aligns with Ndlovu and Demlie (2020) observation that northern KZN had extremely wet conditions in 1995. Ndlovu and Demlie (2020) also stated that there were more extreme dry conditions than wet ones during the historical period, which is mirrored in the outcomes of this study.

### 2.5.3. Future climate projections

The precipitation projections under both RCP4.5 and RCP8.5 scenarios were obtained from the NASA Earth Exchange Global Daily Downscaled Climate Projections dataset (NEX-GDDP; Thrasher et al., 2012) via the Google Earth Engine. The NEX-GDDP dataset comprises of "statistically downscaled climate scenarios for the entire globe at a spatial resolution of 0.25° (~25 by 25 km), derived from 21 Global Climate Model (GCM) runs conducted under Phase 5 of the Coupled Model Intercomparison Project (CMIP5). The NEX-GDDP dataset provides daily estimates of precipitation and temperature (maximum and minimum) for the historical period (1950–2005) and the future period (2006–2099) over the entire globe" (Thrasher et al., 2012). From the ensemble of projections derived from 21 GCMs, the six selected GCMs used in this research are listed in Table A.3.

The selection was done by statistically comparing precipitation trends between each GCM's historical data and the corrected CHIRPS dataset from 01/01/1990–31/12/2005, using the coefficient of determination ( $R^2$ ).  $R^2$  represents the goodness of fit between the observed and simulated data. For  $R^2$ , a range of 0.5–1.0 represents a good agreement between observed and simulated values. The selected GCMs' precipitation outputs achieved the highest  $R^2$  values, which ranged from 0.96 to 0.99, as observed in Figure A.1, thus deeming them satisfactory.

The monthly historical rainfall data from 01/01/1990–31/12/2005 of the selected GCMs, including their RCP4.5 and RCP8.5 projection data from 01/01/2006–31/12/2019, were also bias-corrected using the LS method. The resulting trends are observed in Figs. A.2 to A.5. The scaling factor for each GCM model under each RCP scenario was factored into their respective projected precipitation data from 01/01/2020–31/12/2099.

### 2.5.4. Physical data

The BR catchment was delineated into four local municipalities (LMs), viz. (a) Newcastle, (b) Utrecht, (c) Dannhauser and (d)

Nquthu. Physical data inputs included the population capacity and growth rate per LM, as given in Table A.4. Regarding land use characteristics, only irrigated agricultural land area per LM was accounted for, and are listed in Table A.4. The irrigated areas per crop type, as seen in Fig. A.6, were kept constant throughout the study period.

#### 2.5.5. Hydrologic data

The hydrologic parameters used in this study were surface water abstractions ( $W_A$ ) and reference evapotranspiration ( $ET_R$ ). To quantify  $W_A$  for each LM within the BR catchment, annual water requirements for each WTP were used, together with domestic, irrigation and energy production water demands. Water requirement data for each WTP and the Majuba power station was obtained from uMgeni (2020). Table A.5 displays each municipality's population's annual domestic water requirements, which were used to compute the total domestic water consumption of the catchment. Maize, wheat, oats, soybeans, and ryegrass are the dominant irrigated crops across all LMs (DARD, 2015; StatsSA, 2017) as seen in Figure A.6, with the irrigation water requirements per crop tabulated in Table A.6. For this study, irrigation water requirements per crop type per hectare were assumed constant throughout the study period.

In computing the maximum evapotranspiration ( $ET_C$ ) for irrigated crops,  $ET_R$  and crop coefficients ( $K_C$ ) were used (see Eq. A.1). Due to ease of use and availability,  $ET_R$  data was obtained from the MODIS 16 Global Terrestrial Evapotranspiration Product (MOD16) via Google Earth Engine. The MOD16 global evapotranspiration data is available at a 1 km<sup>2</sup> resolution across the 109.03 million km<sup>2</sup> vegetated land area at 8-day, monthly and annual intervals (Jiang et al., 2020).

For the BR catchment, the 8-day  $ET_R$  data, which was the only dataset available in the Google Earth Engine, ranged from the period 01/01/2001–31/12/2014, as seen in Figure A.7. The 8-day  $ET_R$  is the sum of  $ET_R$  during these 8-day periods in 0.1 kg m<sup>-2</sup>; thus, a conversion factor of 0.1 was applied to obtain  $ET_R$  values in mm per 8 days (Jiang et al., 2020). The data was replicated to cover the period of 1990–2099 under all climate change scenarios, as per Figure A.8, with an average value of 549.82 mm/annum. Monthly  $K_C$  values were obtained from Savva and Frenken (2002), and provided in Table A.7. The largest  $K_C$  value was considered in months when more than one crop was planted.

In determining the actual evapotranspiration ( $ET_A$ ), which is the amount of water consumed by evapotranspiration in the catchment, including water supplied by irrigation, the effective precipitation is initially determined. Effective precipitation percentage ( $P_{eff}$  (%)) is the annual percentage of precipitation available for evapotranspiration; the remainder contributes to surface runoff. WEAP initially assumes a value of 100 % for  $P_{eff}$  (%), i.e., all precipitation is available for evapotranspiration. For this study, as part of calibrating and evaluating the WEAP model (see Section 2.6),  $P_{eff}$  (%) values were adjusted such that the historical streamflow closely matched the catchment's observed streamflow from 1990 to 2019. Using Equation A.2, the average effective precipitation depth ( $P_{eff}$ ) was computed by the WEAP model. Therefore, in determining the  $ET_A$ , the WEAP model selects the minimum value between the  $ET_C$  and the  $P_{eff}$ . The average  $ET_A$  was 496 mm/annum for the historical period, lower than that estimated by DWS (2015) of 802 mm/annum. This is consistent with the assumption that irrigated areas and crops remained unchanged during the study period.

Reservoir storage data, such as storage capacity, reservoir elevation, net evaporation, and surface area, is also important in computing storage changes ( $\Delta S$ ). As there are many reservoirs within the BR catchment, it was impossible to simulate all reservoirs' operations; therefore, it was decided that only government-registered dams should be considered. The above-mentioned data are tabulated in Tables A.8 and A.9.

## 2.6. Model calibration, validation and data analyses

As previously mentioned, the model was calibrated to produce acceptable streamflow simulations by fine-tuning  $P_{eff}$  (%) from 1990 to 2019 (Sieber, 2015). The adopted annual variations of  $P_{eff}$  (%) for all bias-corrected GCM's precipitation are displayed in Fig. A.9. The  $P_{eff}$  (%) variations were replicated throughout the study period.

During the calibration process, monthly CHIRPS and GCM's average ensembles' simulated streamflow were compared with the observed streamflow from 01/01/1990–31/12/2019, obtained from Station V3H010 (Buffels River @Tayside) at latitude 28°3'33.55" and longitude 30°22'24.13" (DWS, 2018). For the validation process, the precipitation dataset used as input to validate the model was statistically compared with the precipitation used in the calibration process to ensure that there is uniformity in the two datasets. In carrying out the statistical analysis, the statistical Welch test for parametric t-tests and the Mann-Whitney test for non-parametric t-tests (Mauser et al., 2015) were used, after checking for the assumption of normality using the Shapiro-Wilks test (Gyamfi et al., 2016). The t-tests were carried out fixing the probability ( $\alpha$ ) at 5 %, so that the null assumption (the means do not differ) is rejected where this is true.

The observed streamflow data used to validate the model was obtained from Station V3H033 (Buffels River Return Flow @Schurvepoort) at latitude 27°36'9.65" and longitude 29°56'33.07" (DWS, 2018), and it was compared with the simulated streamflow data from 01/01/1994–31/12/2002. The study applied the following statistical criteria in the evaluation process: normalised root-mean-square error ( $nRMSE$ ), Willmott's (1981) index of agreement ( $d$ ), percent bias ( $PBIAS$ ) and the  $R^2$  to assess the model's performance. The selected criteria are defined by Eqs. A.3 to A.6, and in Table A.10.

The error index  $nRMSE$  shows the model's performance; however, it does not indicate the degree of over- and under-estimation. Thus,  $d$  was employed to detect additive and proportional differences between observed and simulated means. However, due to the squared differences,  $d$  is over-sensitive to extreme values (Moriassi et al., 2007). The  $PBIAS$ , which measures the average tendency of the simulated data to be larger or smaller than their observed counterparts, was further utilised. The optimal value of  $PBIAS$  is 0%, with low values showing that the model simulation is credible. Positive values indicate under-estimation bias, and negative values indicate over-estimation bias. A  $d$  of 1 indicates a perfect agreement between measured and predicted values, and 0 indicates no agreement.

(Moriasi et al., 2007).

Descriptive statistics such as means, percent increases relative to the historical scenario, and coefficients of variation were used to analyse the model’s output data. The Welsh parametric and the Mann-Whitney non-parametric t-tests were also carried out to analyse and compare data variability, and in cases where three or more datasets were being compared, one-way ANOVA tests were performed (Kim, 2017). Box and whisker plots were also employed to analyse outputs as they can demonstrate dataset stability and general distribution. The variations of the minimum and maximum rainfall across the catchment are displayed by the heights of the box plots, with the median value shown by the line in the middle of the box plots, and outliers indicated by the dots above and/or below the boxplots.

### 3. Results and discussion

#### 3.1. Precipitation

From the box-and-whisker plots in Fig. 4 and Fig. 5, it is evident that the selected GCMs’ bias-corrected historical precipitation data follow the trend and spread of the CHIRPS dataset for the RCP4.5 and RCP8.5 scenarios, except for the CNRM-CM5 model which over-simulated the dispersion and extreme rainfall events of the catchment.

For the RCP4.5 scenario, as per Fig. 4, the projected precipitation trends coincide with the DEA (2013b)’s RCP4.5 statistically downscaled projections for eastern South Africa, where significant increases in BR catchment’s rainfall magnitude and variability were projected in the far future. However in the near- and mid-future, rainfall patterns are unclear and indicate a general mixed-signal of wetter or drier conditions, depending on the GCM used. Under the RCP8.5 scenario, as seen in Fig. 5, similar projections of average increases are found throughout the study period. However, the near-future scenario is the exception, where 5 out of 6 GCMs projected a decline in precipitation compared with the CHIRPS data.

To investigate the overall projected climate changes in the BR catchment, the multi model ensemble mean approach was adopted

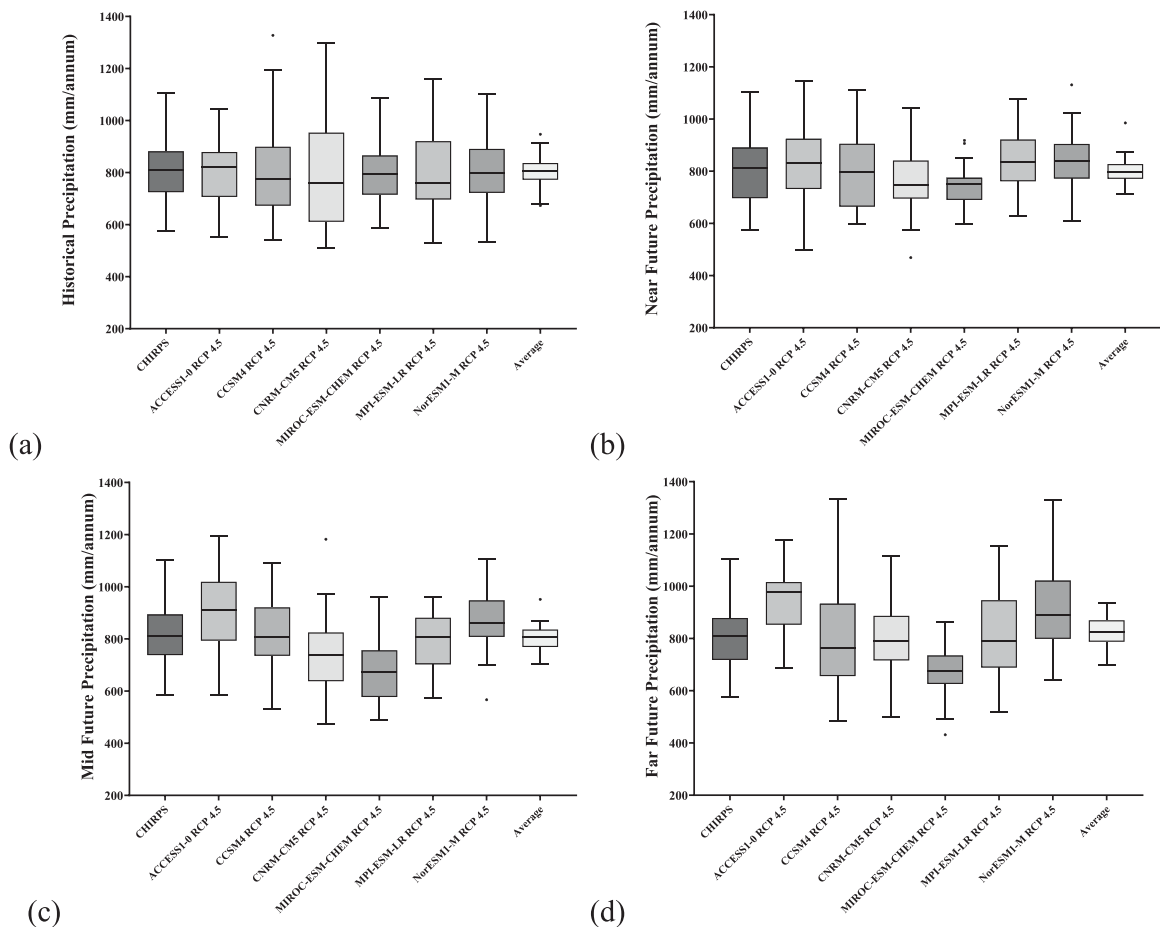
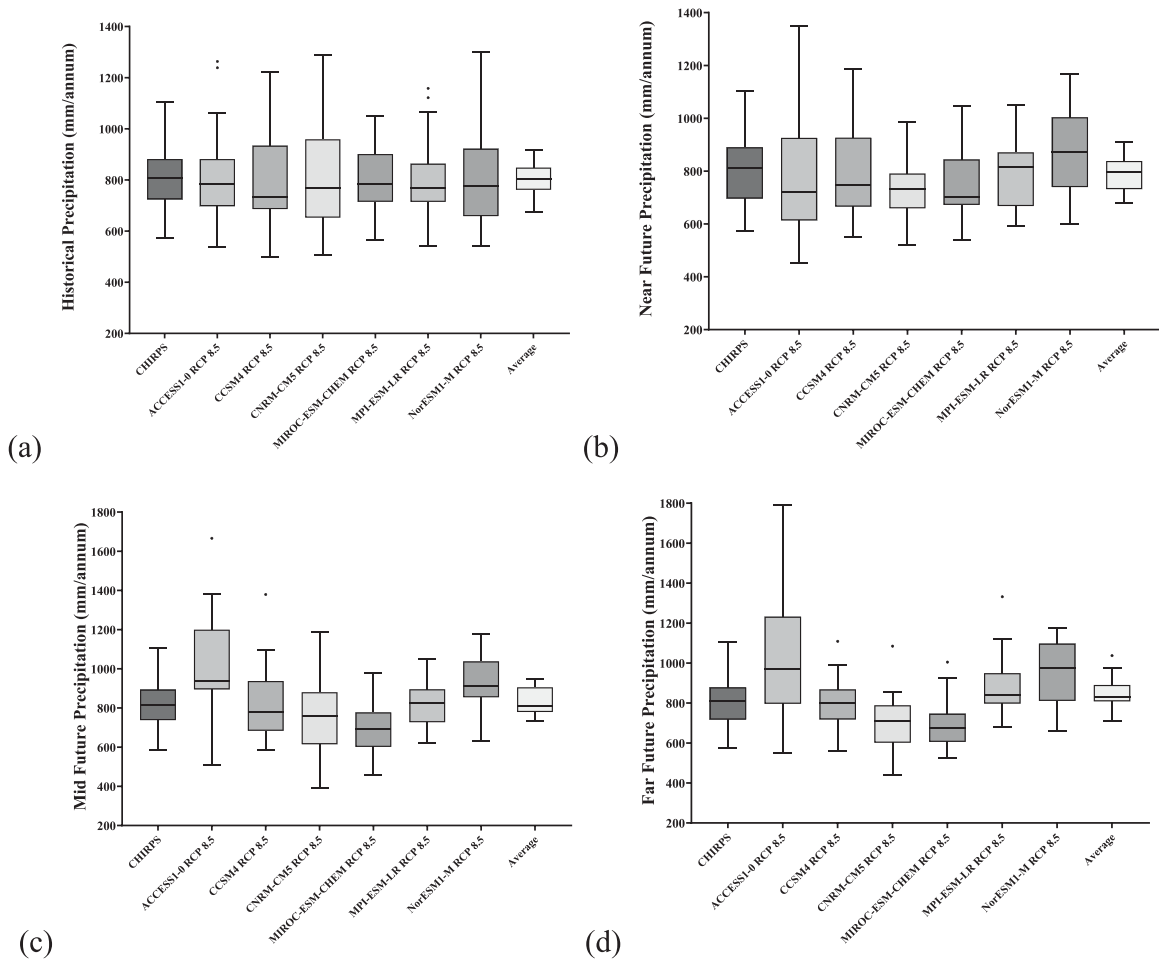


Fig. 4. Comparison of the Buffalo River catchment’s bias-corrected GCM average annual precipitation (mm/annum) outputs during the historical (a), near future (b), mid-future (c) and far future (d) timeframes under the RCP4.5 scenario, with CHIRPS representing the historical remote sensed precipitation. In graphs (b) to (d), CHIRPS dataset is for comparison purposes only.



**Fig. 5.** Comparison of the Buffalo River catchment’s bias-corrected GCM average annual precipitation (mm/annum) outputs during the historical (a), near future (b), mid-future (c) and far future (d) timeframes under the RCP8.5 scenario. In graphs (b) to (d), CHIRPS dataset is for comparison purposes only.

(Tramblay et al., 2018; Hadri et al., 2022), whereby the projected changes of the 6 GCMs were averaged annually under both RCP4.5 and RCP8.5 scenarios. In the near- and mid-future periods, the average ensemble of the RCP4.5 scenario projected precipitation to remain within the historical range, with MAP increases of 0.06 % and 0.32 %, respectively. Decreases in variability are also modelled in the aforementioned timeframes for RCP4.5, shown by the coefficient of variation (CV) decreasing slightly from a historical value of 7.9–6.5 % and 6.7 %, respectively. However, for the far-future timeframe, a slight increase in rainfall is projected as the percent increase of MAP is 3.4 %. Increased variability is also noted by the CV value increasing to 7.1 %.

The average ensemble of the RCP8.5 scenario projected a slight decrease in the amount of precipitation received by the catchment in the near future, with a MAP percentage decrease of – 2 %, resulting in an overall MAP value of 787 mm. The rainfall variations amplified slightly during this timeframe as the CV increased from a historical value of 7.9–8.1 %. Increases in precipitation magnitude and fluctuations in the mid- and far-future are more prominent than in the RCP4.5 scenario, with the percentage increase of MAP being 4.3 % and 5.4 %, respectively, and the CV value reaching 8.5 % in both periods. From the box-and-whisker plot in Fig. 6, a positive skewness resulted in the far future, signifying that the frequency of low rainfall occurrences ( $\leq 825$  mm, lower than the average of 845 mm) is expected to increase. It is also important to highlight the widened lengths of the 75th and 90th quartile whiskers in the far-future, which reflect an anticipated increase in the magnitude of extreme wet events.

A statistical analysis was carried out to compare the GCMs precipitation output ensembles for RCP4.5 and RCP8.5, shown in Table 2. Findings indicated that there is no significant difference between the scenarios results. Furthermore, one-way ANOVA Kruskal-Wallis tests were run to examine if there is any significant variability in the data (Kruskal and Wallis, 1952) from each RCP scenario’s four timeframes: historical, near-future, mid-future, and far-future. The RCP4.5 produced a p-value of 0.255, indicating that there is no significant difference within its dataset throughout the study period. The RCP8.5 scenario, on the other hand, yielded a p-value of 0.01, indicating a significant difference within its dataset, attributable to its mid- and far-future fluctuation increases.

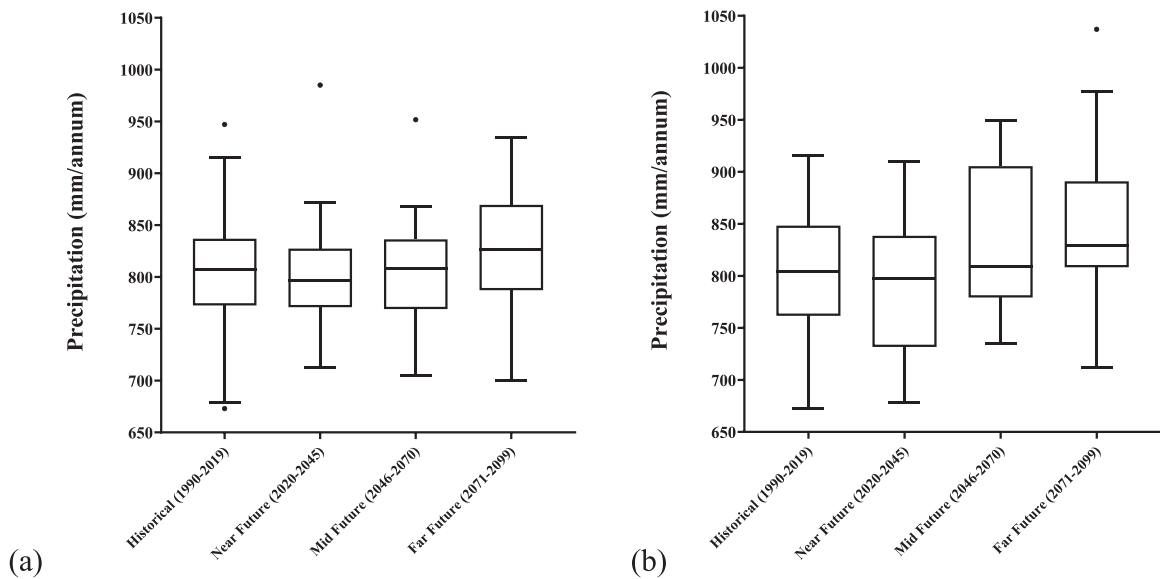


**Fig. 6.** Distribution of average annual precipitation (mm/annum) for the average ensembles during the historical (1990–2019), near future (2020–2045), mid-future (2046–2070), and far future (2071–2099) timeframes under the RCP4.5 scenario (a) and the RCP8.5 scenario (b) in the Buffalo River catchment.

**Table 2**

Statistical analysis of the RCP4.5 and RCP8.5 GCMs annual precipitation (mm/annum) ensemble for the Buffalo River catchment during the historical (1990–2019), near future (2020–2045), mid-future (2046–2070) and far future (2071–2099) timeframes.

Ensemble of Climate Output Data (mm/annum)	Shapiro-Wilk Normality ( <i>p</i> -value)	Welsch t-test p-value	Mann-Whitney t-test p-value	Differences in Means (Welsch) or Medians (Mann-Whitney)	Significance Results
Historical RCP4.5	Yes (0.292)	0.967	-	0.702	Not Significant
Historical RCP8.5	Yes (0.759)	-	-	-	-
Near Future RCP4.5	No (0.004)	-	0.429	1.105	Not Significant
Near Future RCP8.5	Yes (0.50)	-	-	-	-
Mid-future RCP4.5	Yes (0.517)	-	0.224	0.310	Not Significant
Mid-future RCP8.5	No (0.03)	-	-	-	-
Far Future RCP4.5	Yes (0.497)	0.346	-	16.42	Not Significant
Far Future RCP8.5	Yes (0.628)	-	-	-	-

### 3.2. Evapotranspiration

Actual evapotranspiration ( $ET_A$ ) was the largest component of the water budget represented by the model. Fig. 7 shows that low  $ET_A$  values are under-simulated for all GCM models compared to the CHIRPS dataset. Overall, the average ensembles of  $ET_A$  projections under RCP4.5 and RCP8.5 scenarios maintained a value of 4500  $Mm^3/annum$ . Small declines in  $ET_A$  are only noted in the near future under the RCP8.5 scenario as the percentage decrease was  $- 2\%$ , this being a consequence of the decline in precipitation projected in the same timeframe.

There is a strong correlation between precipitation and  $ET_A$  fluctuations. For the RCP4.5 scenario, the  $ET_A$ 's CV declined from a historical value of 10–7.5% and 7.9% in the near- and mid-future, respectively. However, the  $ET_A$ 's CV increased to 9% in the far-future. The RCP8.5 scenario's CV slightly increased in the near future from a historical value of 8.5–8.6%, and then it declined in the mid- and far-future to 8.1% and 8.4%, respectively; the decline is to be noted as a result of the increased frequency of low precipitation events.

### 3.3. Surface runoff and streamflow

When compared to the surface runoff ( $R$ ) simulated using the CHIRPS historical precipitation, Fig. 8 shows over-simulated  $R$  values under both RCP4.5 and RCP8.5 scenarios. The over-simulation is, however, statistically insignificant; after performing the Shapiro-Wilk normality test, all three datasets exhibited a normal distribution. The Welch's ANOVA F-test (Liu, 2015) was therefore performed on the CHIRPS, and all GCM output data, which produced a p-value of 0.17.

For  $R$  projections, as seen in Figs. 9 and 10,  $R$  is constant throughout the study period under the RCP4.5 scenario, with an average

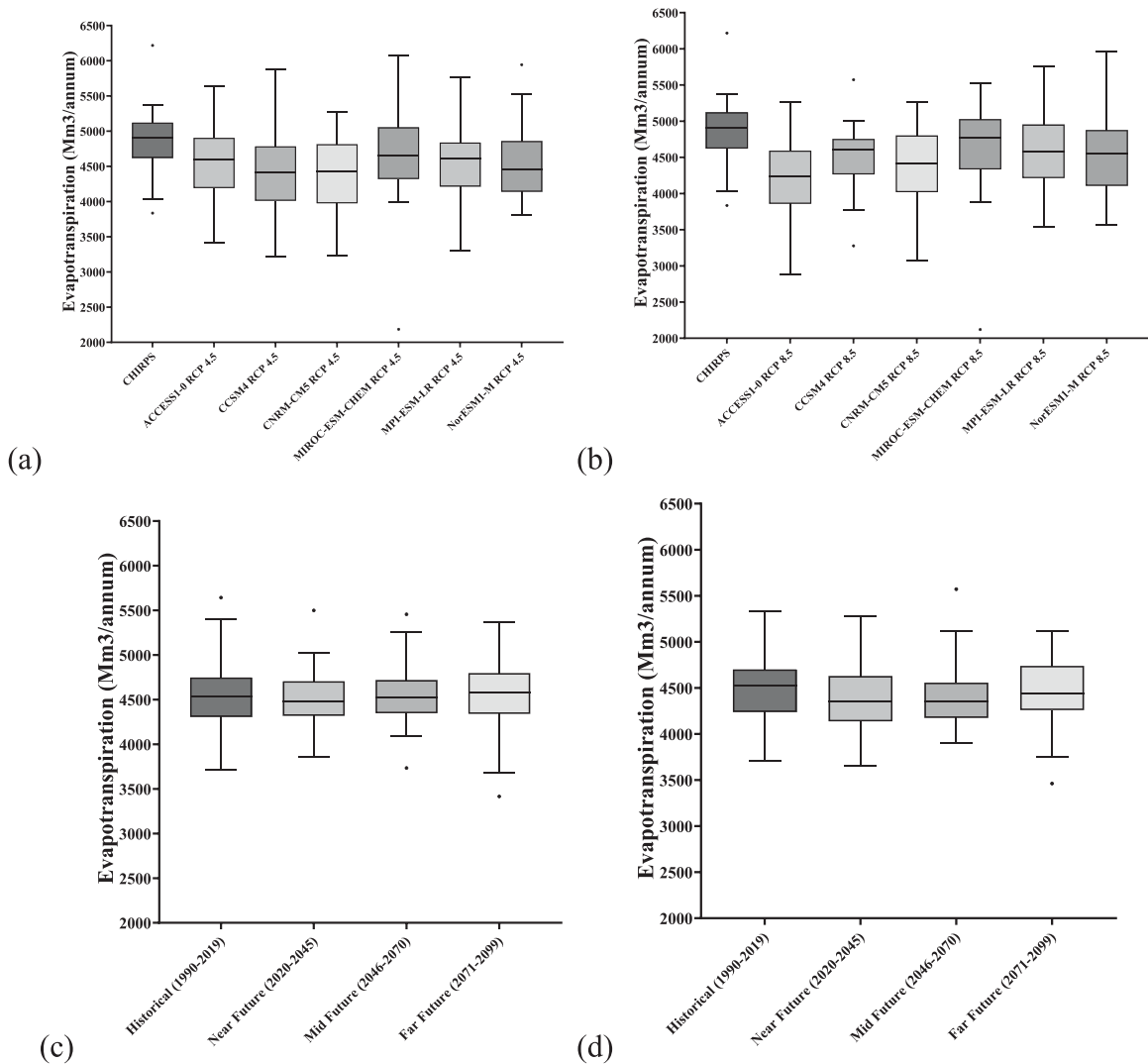


**Fig. 7.** Comparison of the Buffalo River catchment’s simulated GCM average annual actual evapotranspiration ( $ET_A$ ) ( $Mm^3/annum$ ) during the historical period (1990–2019) under the RCP4.5 scenario (a) and RCP8.5 scenario (b), and distribution of simulated  $ET_A$  by average ensemble throughout the study period (2020–2099) under the RCP4.5 scenario (c) and RCP8.5 scenario (d).

value of  $3330 Mm^3/annum$ . However, significant increases are observed in the far-future, with the mean  $R$  being  $3566 Mm^3/annum$ . The CV displays a decreasing trend as it dropped from a historical value of 19 %, to 17 % in the near future, and 15 % in both the mid- and far future timeframes.  $R$  projections under the RCP8.5 scenarios display decreasing fluctuations in the near future; the CV dropped from a historical value of 19–16 %; however, the mean remained unchanged as it is  $3315 Mm^3/annum$ . For the mid- and far-future, notable increases in both magnitude and fluctuations are projected: the mean values increased by 0.6 % and 8 % to  $3698$  and  $3815 Mm^3/annum$ , respectively, and the CV also increased to 21 % and 17 %, respectively.

After computing surface water abstractions ( $W_A$ ) which are discussed in Section 3.4, and return flows, a streamflow graph was produced by the WEAP model of each river’s nodes and reaches. In the water balance computation, the streamflow at the BR’s outlet ( $Q$ ) is considered. Projections for  $Q$  values under the RCP4.5 scenario display slight increases in the near- and mid-future, as the annual averages increase from a historical value of  $3028 Mm^3/annum$  to  $3034$  and  $3046 Mm^3/annum$ , respectively. As per the precipitation and  $R$  projection trends,  $Q$  also increased rapidly in the far-future, with the percentage increase shooting up from a mid-future value of 0.6–8 % in the far future, and the annual average  $Q$  being  $3267 Mm^3/annum$ .

The RCP8.5 scenario displays the highest  $Q$  averages under the mid- and far-future timeframes, as seen in Fig. 11. A very slight decline by 2 % in the annual average  $Q$  is projected in the near future, from a historical value of  $3081–3024 Mm^3/annum$ . Moreover, increases by 13 % and 14 % are projected in the mid- and far-future timeframes, respectively. These increases in magnitude were accompanied by increased fluctuations as the CV increased from 17 % in the near-future, to 22 % and 18 % in the mid- and far-future, respectively. The box-and-whisker plot for the far future timeframe also displays a positive skewness of 1.105, indicating anticipated

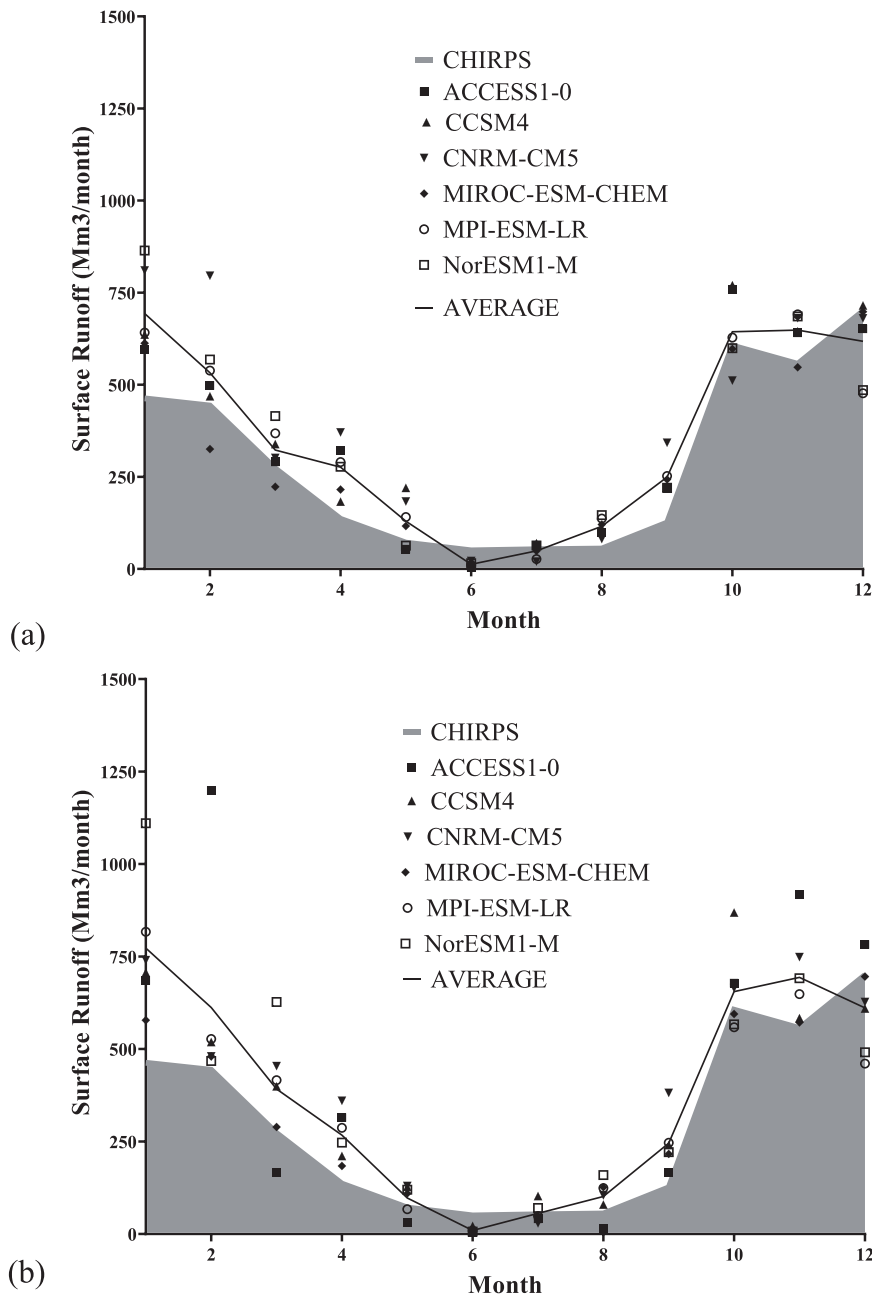


**Fig. 8.** Comparison of the spread of average monthly simulated surface runoff ( $R$ ) ( $Mm^3/month$ ) by CHIRPS data and all GCMs under the historical period (01/01/1990–31/12/2019) for the RCP4.5 scenario (a) and RCP8.5 scenario (b) in the Buffalo River catchment.

increased events of high-value streamflow exiting the catchment. This is mainly attributed to increased precipitation values, as well as low magnitude and variability in  $ET_A$  values during this period. These results are consistent with the research findings by [Graham et al. \(2011\)](#), [DEA \(2013a\)](#) and [Schütte et al. \(2022\)](#), which projected that the RCP8.5 CC scenario would increase  $Q$  in KZN.

### 3.4. Water abstractions

As previously mentioned, in addition to  $ET_A$  and  $Q$ ,  $W_A$  were considered an outflow component of the water balance. The BR system’s bulk water supplies (WTPs), were modelled to require  $63 Mm^3/annum$  in order to function at their optimum capacity, as seen in [Fig. B.1](#), similar to the [uMgeni \(2019\)](#); [uMgeni \(2020\)](#) value of  $61.8 Mm^3/annum$ .

The total primary water demands that the BR system’s WTPs transfer water to, i.e., energy production, domestic, and irrigation water demands, were estimated to increase from approximately  $108 Mm^3/annum$  in 1990, to  $197 Mm^3/annum$  in 2099, as per [Fig. 12](#).

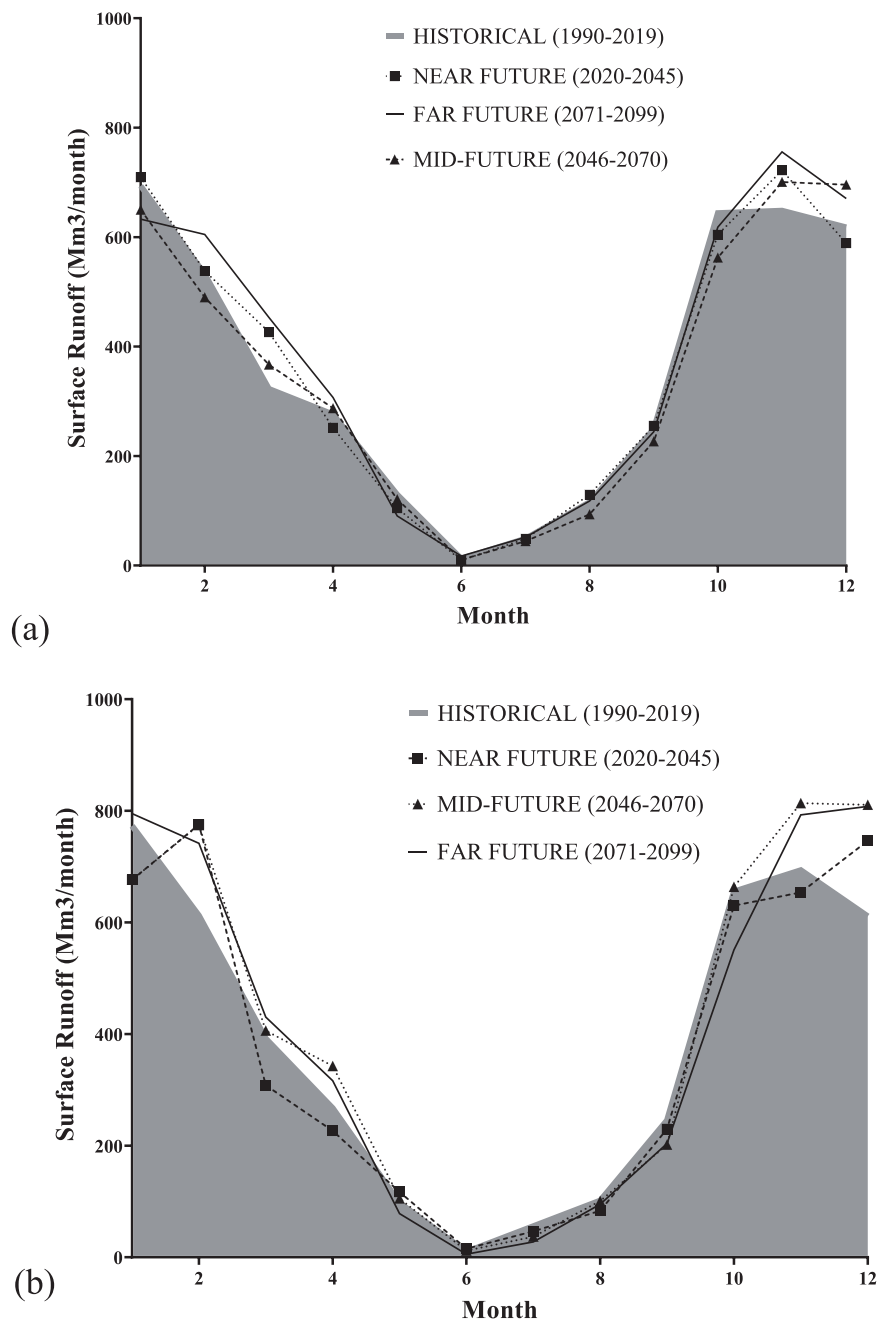


**Fig. 9.** Comparison of the spread of monthly simulated surface runoff ( $R$ ) ( $Mm^3/month$ ) by the average ensemble under the historical (01/01/1990–31/12/2019), near future (01/01/2020–31/12/2045), mid-future (01/01/2046–31/12/2070) and far-future (01/01/2071–31/12/2099) timeframes for the RCP4.5 scenario (a) and RCP8.5 scenario (b).

Domestic water demands, which were projected to increase in line with the LMs’ population growth rates, produced satisfactory and similar results when compared to study findings from recent reports, as shown in Table 3. It should be noted that, for the Nquthu LM, only Area 2 and Area 5 are dependent on the BR catchment for water supplies (Shabalala and Mthembu, 2022).

Of the above-mentioned water demands, the average  $W_A$  from the BR catchment’s raw water supplies i.e., rivers and reservoirs, range from  $113 Mm^3/annum$  to  $115 Mm^3/annum$ , as per Fig. 13. When taking a closer look at the monthly distribution of these  $W_A$  under the worst-case climate change scenario (RCP8.5), also seen in Fig. 13, approximately 40 % constitute of water supplied to the Ngagane WTP, mainly because it is the primary supplier of numerous water demand sites in the catchment, including the densely populated Newcastle LM. Also, the Majuba Power Station abstracts 100 % of its water demands, which are approximately 23 % of  $W_A$ , due to it being the primary demand site assigned at the Zaaiohoek Dam. In terms of LMs, Newcastle is expected to extract the majority of

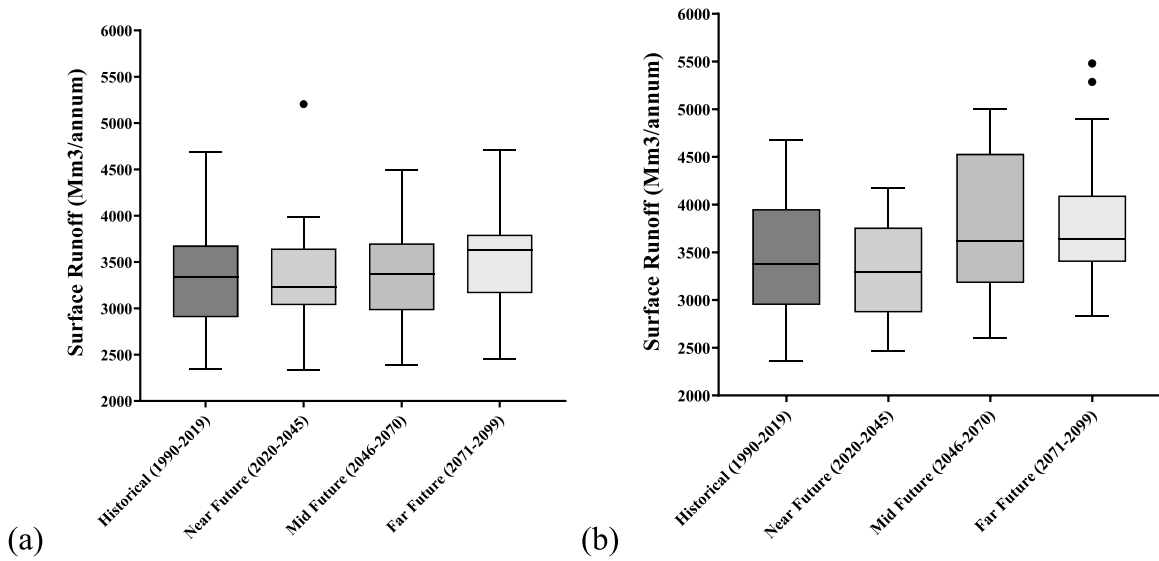


**Fig. 10.** Distribution of simulated average annual surface runoff ( $R$ ) ( $Mm^3/annum$ ) for the average ensemble during the historical (1990–2019), near future (2020–2045), mid-future (2046–2070), and far future (2071–2099) timeframes under the RCP4.5 scenario (a) and the RCP8.5 scenario (b).

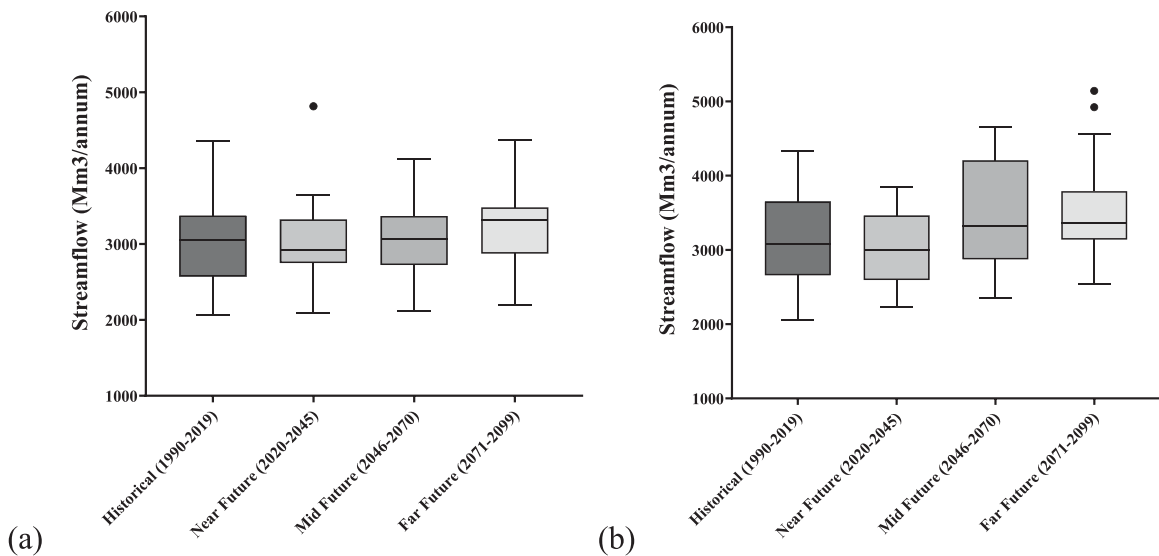


**Fig. 11.** Distribution of simulated average annual streamflow ( $Q$ ) at the Buffalo River's outlet ( $Mm^3/annum$ ) for the average GCM ensemble during the historical (1990–2019), near future (2020–2045), mid-future (2046–2070), and far future (2071–2099) timeframes under the RCP4.5 scenario (a) and the RCP8.5 scenario (b).

water supplies, which is attributable to its rapidly increasing population that forms 53 % of the total domestic water demands. Such outcomes are also reflected under the RCP4.5 climate scenario, as per Fig. B.2.

With the BR system only allowing maximum  $W_A$  of  $118 Mm^3/annum$  throughout the study period, as per Fig. 13 and B.9, unmet demands are therefore anticipated to be exacerbated in the catchment, from  $90 Mm^3/annum$  in the historical timeframe to  $135 Mm^3/annum$  in the far future. This is understood to be a result of the limitations imposed by the storage capacity of the BR catchment, which does not capture the increased precipitation received throughout the 21st century, and also confirms findings from the *uMgeni* (2020), which state that the BR catchment's water storage capacity is not sufficient to provide the increasing demands of the catchment.

### 3.5. Changes in surface water store

The hydrological water balance components for the BR catchment developed from the WEAP model under the RCP4.5, and RCP8.5

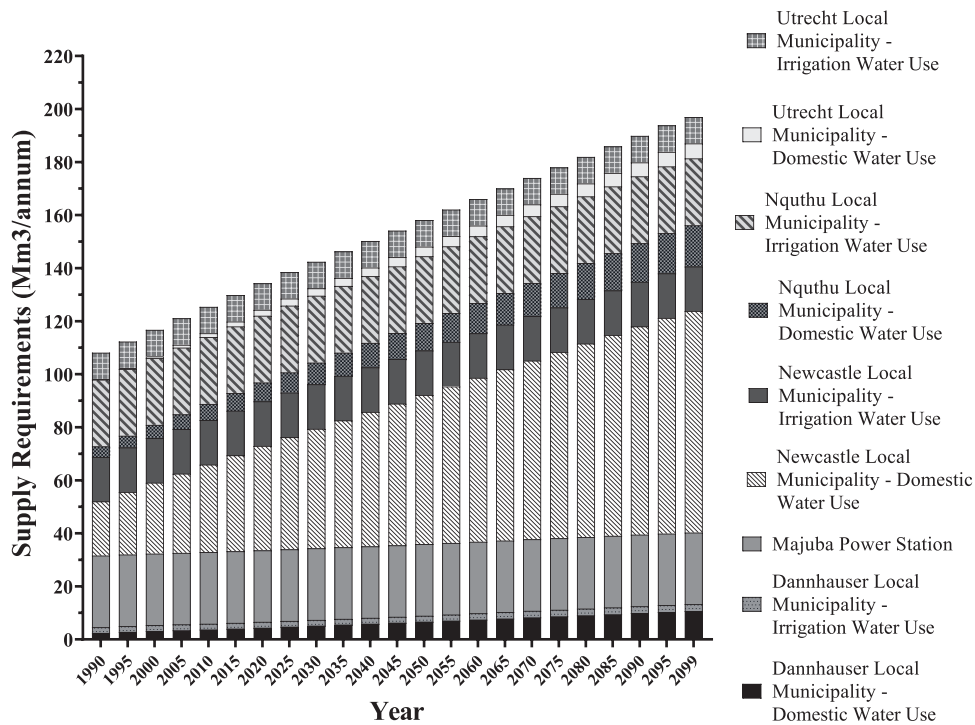


Fig. 12. Total annual supply requirements (Mm<sup>3</sup>/annum) of the local municipalities within the Buffalo River catchment, and the Majuba power station, throughout the study period (1990–2099).

Table 3

Comparisons of projected domestic water demands per local municipality (Mm<sup>3</sup>/annum) in the Buffalo River catchment using the WEAP model, and from recent studies for years 2020–2050.

Local Municipality	Projected Domestic Water Demands (Mm <sup>3</sup> /annum)					Source (s)
	2020	2025	2030	2035	2050	
Newcastle	39.34 (39.34)	42.25 (42.25)	45.36 (45.04)	47.83 (47.83)	-	(uMgeni, 2016)
Dannhauser	5.66 (4.41)	6.30 (4.78)	7.00 (5.16)	7.52 (5.54)	-	
Utrecht	1.86 (2.25)	2.25 (2.63)	2.63 (2.84)	2.87 (3.04)	-	
Nquthu (Area 2 and 5)	7.12 (7.12)	7.54 (7.65)	8.08 (8.19)	-	10.31 (10.32)	(uMgeni, 2020, 2021)

\*Italised values were projected in this study using the WEAP model

scenarios are summarised in Tables B.1 and B.2, respectively. When compared to the historical surface water storage ( $S_N$ ) trends simulated with the CHIRPS data which yielded a CV of 28.9 %, both RCP4.5 and RCP8.5 historical average ensembles displayed slightly lower variations (see Fig. 14), with the CV being 22 %. This is due to the average ensembles’ precipitation values, under both RCP scenarios, also consisting of lower fluctuations than the CHIRPs historical average.

From Fig. 15, and also in Tables B.1 and B.2, the annual projections of  $S_N$  indicate slight increases in magnitude and decreased variations, more so in the far future, whereby the average  $S_N$  is expected to increase by 8% under both climate scenarios relative to the historical average of 260 Mm<sup>3</sup>/annum, and CV values are projected to decline by 7 % and 8 % under the RCP4.5 and RCP8.5 scenarios, respectively. This is also anticipated as a result of increased precipitation, which is likely to increase the frequency with which reservoirs are recharged. However, as also observed in Fig. 15, these changes in water storage are similar to those of the historical timeframe and are minimal as compared to the precipitation increases expected towards the end of the 21st century. Such findings also reflect the inadequacies and limitations imposed by the water storage facilities of the catchment in capturing the increased precipitation, causing increased Q and unmet demands throughout the projection period.

### 3.6. Model performance evaluation

The precipitation datasets utilised in the calibration and validation processes displayed no statistical difference, as seen in Table 4, and the performance measures also indicated a very good performance of the WEAP model in the BR catchment for streamflow simulation at a monthly scale. In the first instance of model calibration, the model’s performance was satisfactory, as evidenced by the model performance statistics (Table 5). However, the model over-simulated streamflow under the CHIRPS dataset and the average

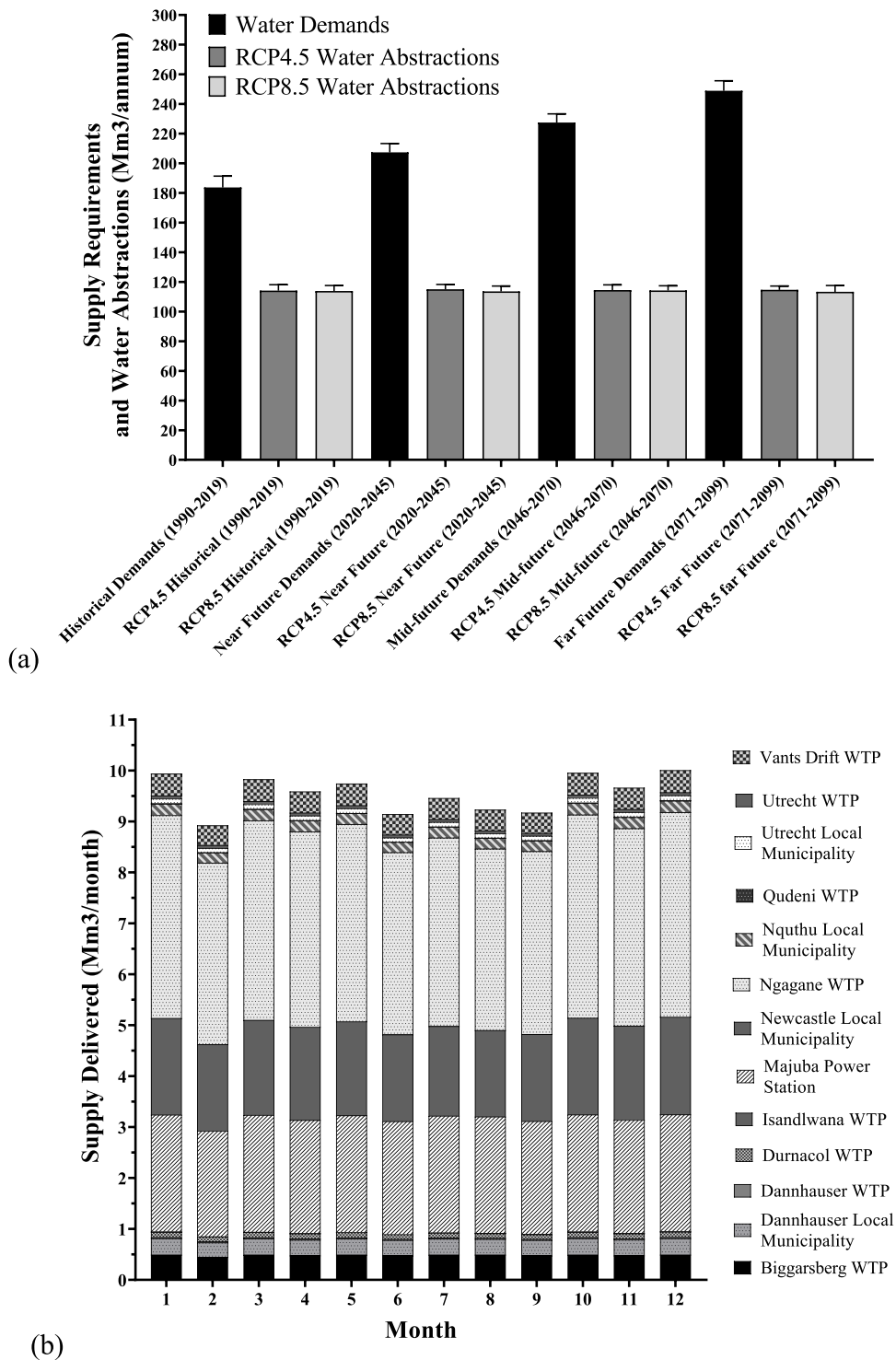


Fig. 13. Total water abstractions (Mm<sup>3</sup>/month) in the Buffalo River catchment (a) per annum from 1990 to 2099 and (b) per month during the RCP8.5 projection period (2020–2099).

ensemble of the GCMs under the RCP4.5 and RCP8.5 scenarios, as seen in Fig. 16. This is also indicated by the *PBIAS* values ranging from  $-19.62$  to  $-24.17$ . The over-simulation could be attributed to the use of 8-day  $ET_A$  data in the water balance computation, which had to be disaggregated evenly across 8 days to obtain daily  $ET_A$  values. This method of calculating monthly  $ET_A$  values during the data input process could be one of the causes of overestimated streamflow. However, the evaluation statistics all qualify as

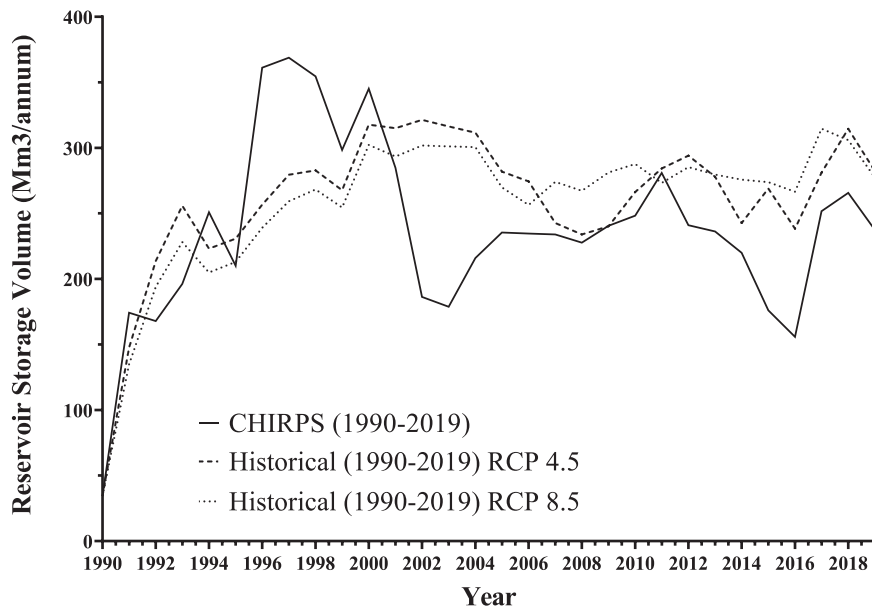


Fig. 14. Historical (1990–2019) annual reservoir storage volume ( $Mm^3/annum$ ) of the Buffalo River catchment under RCP4.5, RCP8.5, and the CHIRPS scenario.

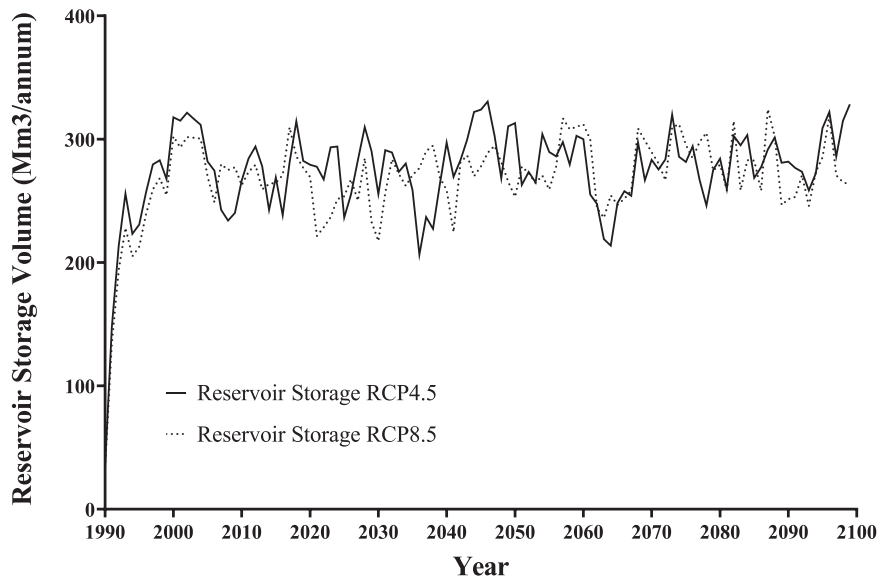


Fig. 15. Distribution of the Buffalo River catchment’s simulated average annual reservoir storage ( $Mm^3/annum$ ) for the average ensembles during the historical (1990–2019), near future (2020–2045), mid-future (2046–2070), and far future (2071–2099) timeframes under the RCP4.5 and the RCP8.5 scenarios.

satisfactory. Under the RCP4.5 and RCP8.5 GCMs’ average ensembles, the model’s simulated streamflow displayed the least correlation when compared to the observed, with the  $R^2$  values being 0.7614 and 0.805, respectively, and the  $nRMSE$  values being 40.77 and 44.25, respectively.

After validation, the model’s performance was deemed to be very good. An improvement in the streamflow simulation was observed, as seen in Fig. 17, which yielded positive  $PBIAS$  values ranging from 8.94 to 18.43. In terms of correlation among the streamflow trends, the model produced streamflow values with improved correlation when compared to the observed as the  $nRMSE$  values decreased from a range of 22.32–44.25 during calibration, to a range of 2.674–5.51.

**Table 4**

Statistical analysis of the CHIRPS, RCP4.5 and RCP8.5 GCMs ensembles precipitation input (mm/month) used to calibrate and validate the WEAP model.

Climate Datasets (mm/month)	Shapiro-Wilk Test	Mann-Whitney Non-parametric T-test		
	Normality ( <i>p</i> -value)	Median Value	P-value	Statistical Significance
CHIRPS Calibration (1990–2019)	No (< 0.0001)	49.73	0.432	Not Significant
CHIRPS Validation (1994–2002)	No (< 0.0001)	56.55		
RCP4.5 GCMs Ensemble Calibration (1990–2019)	No (< 0.0001)	57.98	0.738	Not Significant
RCP4.5 GCMs Ensemble Validation (1994–2002)	No (< 0.0001)	64.93		
RCP8.5 GCMs Ensemble Calibration (1990–2019)	No (< 0.0001)	56.49	0.951	Not Significant
RCP8.5 GCMs Ensemble Validation (1994–2002)	No (< 0.0001)	61.99		

**Table 5**

Calibration and validation statistics of observed vs. simulated streamflow by the CHIRPS dataset and RCP4.5 and RCP8.5 GCMs' average ensembles.

		CHIRPS	RCP4.5	RCP8.5
Calibration Statistics	<i>d</i>	0.958 (VG)	0.860 (VG)	0.836 (VG)
	<i>n</i> RMSE (%)	22.32	40.77	44.25
	PBIAS	-22.54 (S)	-19.62 (S)	-24.17 (S)
	<i>R</i> <sup>2</sup>	0.902	0.7614	0.805
Validation Statistics	<i>d</i>	0.790 (G)	0.951 (VG)	0.832 (VG)
	<i>n</i> RMSE (%)	5.51	2.674	4.933
	PBIAS	18.43 (S)	8.940 (VG)	16.49 (G)
	<i>R</i> <sup>2</sup>	0.905	0.988	0.987

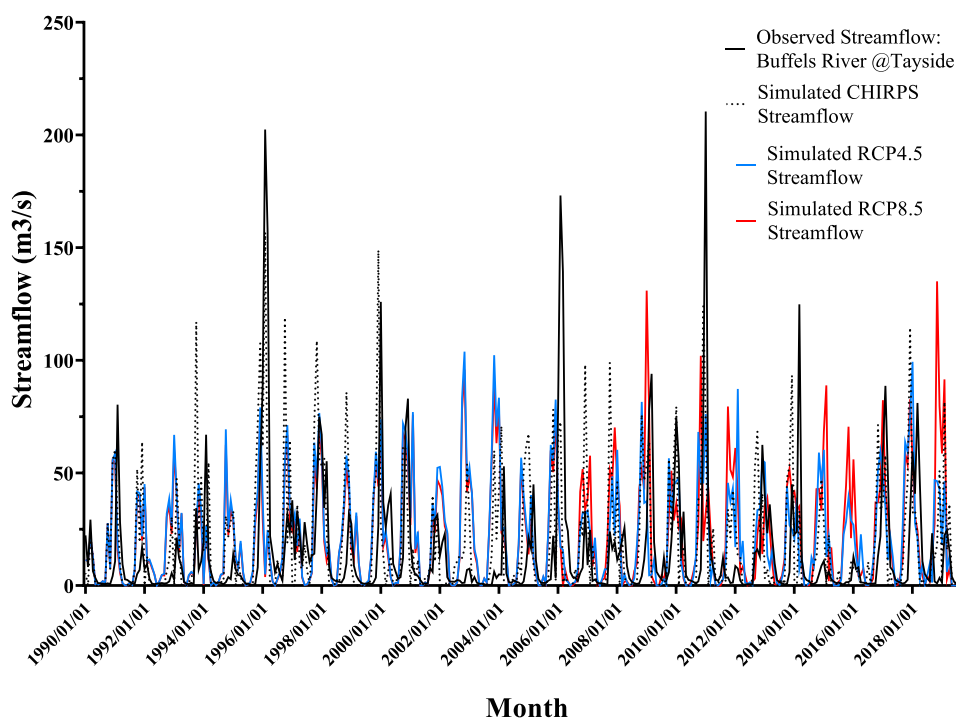


Fig. 16. Monthly simulated versus observed streamflow of the Buffalo River for the calibration period (01/01/1990–31/12/2019).

#### 4. Limitations

According to the study findings, the BR catchment is a high rainfall region expected to receive more rainfall under the RCP8.5 and RCP4.5 scenarios. Using statistically downscaled precipitation projections, which lack high-resolution data to base their downscaling, limits the findings. However, from the WEAP model performance evaluation statistics, the bias-correction method applied to the precipitation projections produced suitable precipitation results reflective of the catchment's hydrology. It is worth remembering that, for the purpose of this study, groundwater recharge was not modelled. Additional limitations include the assumption of uniform

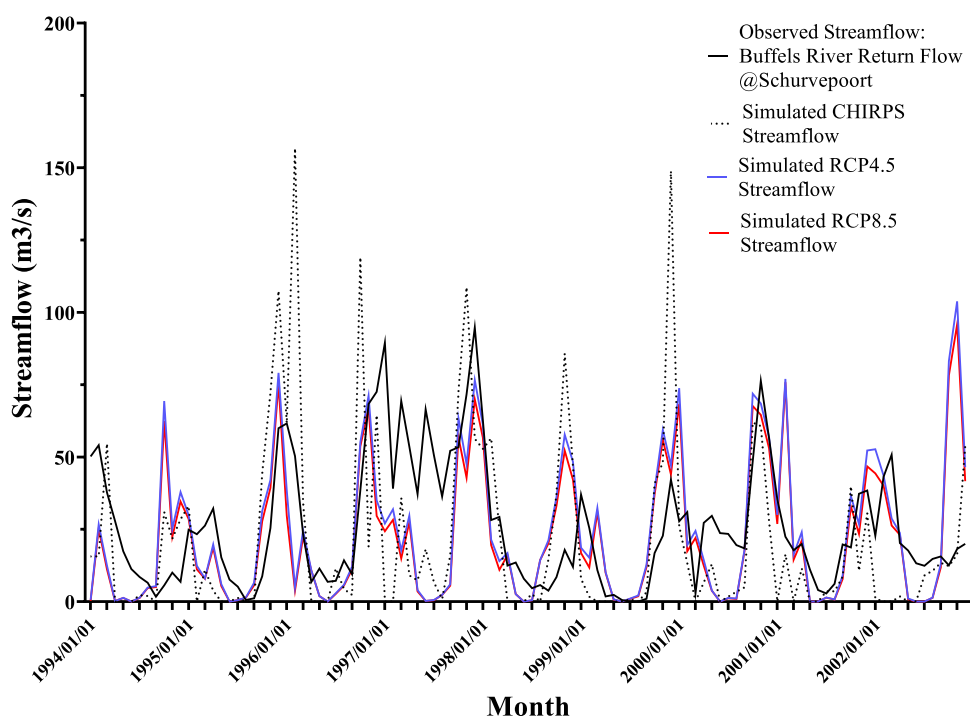


Fig. 17. Monthly simulated versus observed streamflow of the Buffalo River catchment for the validation period (01/01/1994–31/12/2002).

reference evapotranspiration under all scenarios, and constant irrigated areas and irrigation water requirements throughout the study period. As such, these limits must be taken into account when employing the simulated runoff values produced by this WEAP model configuration. As a result, the simulated runoff values are recommended for comparison purposes, including comparing runoff generated under various RCP scenarios, GCMs, and time periods.

## 5. Conclusion and recommendations

The objective of this study was to assess the impacts of climate change on surface water availability in the Buffalo River catchment. Various future scenarios were developed by acquiring the catchment's historical and climate model output data. These were integrated into the WEAP model, which evaluated the catchment's available surface water under all scenarios. The findings under both RCP4.5 and RCP8.5 scenarios are coherent and suggest that mean annual precipitation is expected to increase under climate change, consequently inducing increased evapotranspiration and surface runoff. Increased magnitudes of droughts and floods are also anticipated under climate change, and as such, larger variations in surface runoff and reservoir storage were modelled. Through recharge during periods of peak flood (extreme wet) events, climate change is expected to increase surface water availability. The WEAP model's accuracy depends on the amount of available information and the degree of detailedness. Thus, it is highly recommended that future works improve the accuracy of details used in simulating hydrological processes using the WEAP model.

Even with the increased surface water availability, unmet demands are anticipated to increase in the catchment. The study's results also revealed that the bulk of the catchment's precipitation is converted to evapotranspiration. Surface runoff at the outlet of the catchment is projected to increase under climate change; therefore, it is recommended that the catchment's surface water storage capacity be increased. Water storage capacity can be optimised through the expansion and construction of new water treatment facilities and using various water harvesting technologies such as micro dams, ponds, weirs, and check dams. Such projects do, however, need to take into consideration the maintenance of environmental flows needed to maintain river ecosystems.

In promoting integrated resource management, the WEF nexus approach can be applied in this case for designing multi-purpose reservoirs, which can be operated not only for increased water supply, but also for hydropower generation, maintenance of navigation depths and flood management. Multi-purpose dams also increase irrigation diversions as well as intensifying small-holder agriculture. In planning and designing of multi-purpose reservoirs, there are trade-offs that do need to be addressed, such as the negative effect hydropower generation has on water quality through: (a) increased water temperatures and (b) an altered sediment regime, which consequently disturbs river ecosystems and poses a risk of waterborne diseases. Therefore, applying the WEF nexus approach will assist in detecting trade-offs and formulating strategies that minimise their materialisation.

With CC expected to increase the fluctuation of surface water availability, it is also recommended that integrated catchment management strategies that holistically view land-use interests and understand inherent trade-offs within the system, be put into effect in partnership with water users and the community. This includes discussing and designing management approaches to meet demands

for food production and ecosystem services in the context of limited land resources, climate change and ecosystem degradation. For such, there are significant trade-offs that need to be addressed.

Expansion of agricultural lands to meet short- and long-term societal needs necessitates more land and water, resulting in a larger water footprint, less available water for domestic consumption, and increased deforestation, which deteriorates water quality. Cur-tailing agricultural land expansion would thus require increased yields per hectare, but this might demand rigorous usage of pesticides and fertilisers, which might degrades water quality through run-off and nitrate pollution, and thus plummets the ecosystem's health. The WEF nexus approach could therefore be used to improve food production sustainably through the investigation of technological and policy measures, such as designing conservation and climate smart agricultural techniques and improved irrigation systems focused on increasing water productivity and/or average yield without affecting water quality.

The performance of the WEAP model was assessed statistically, and the results indicate a sufficient model fit. This study's findings illustrate the WEF nexus' CLEW complex relationships, particularly the examined relationship between climate and water availability. In its ability to do so, the WEF nexus has proven capable of systematically analysing, integrating, and managing the challenges brought upon by climate change on water resources in a sustainable manner, through the use of other WEF nexus quantitative and conceptual analytical tools and frameworks.

### **CRedit authorship contribution statement**

Conceptualization: **N Dlamini, A Senzanje and T Mabhaudhi**, Methodology: **N Dlamini, A Senzanje and T Mabhaudhi**, Software: **N Dlamini**, Validation: **N Dlamini, A Senzanje and T Mabhaudhi**, Formal analysis: **N Dlamini, A Senzanje and T Mabhaudhi**, Investigation: **N Dlamini**, Resources: **A Senzanje and T Mabhaudhi**, Data Curation: **N Dlamini**, Writing – Original Draft: **N Dlamini**, Writing – Review & Editing: **A Senzanje and T Mabhaudhi**, Visualization: **N Dlamini**, Supervision: **A Senzanje and T Mabhaudhi**, Project Administration: **A Senzanje and T Mabhaudhi**, Funding Acquisition: **T Mabhaudhi**.

### **Declaration of Competing Interest**

The authors declare that they have no known competing financial interests or personal relationships that could have appeared to influence the work reported in this paper.

### **Data availability**

Data will be made available on request.

### **Acknowledgement**

The authors thank Dr Serge Kiala for his assistance gathering hydrological and climatological data. The authors are thankful to Dr Carole Dalin from University College London, Mr Richard Kunz, and Dr Stefanie Schütte from the University of KwaZulu-Natal for providing valuable input and direction during the critical review and redrafting. The first author is thankful to the National Research Fund (NRF) and the Nurturing Emerging Scholars Programme (NESP) for financial support. This work was funded by the Water Research Commission (WRC K5/2967//4). This work forms part of the Sustainable and Healthy Food Systems (SHEFS) Programme, supported through the Wellcome Trust's Our Planet, Our Health Programme [grant number: 205200/Z/16/Z]. This work was also carried out as part of the Nexus Gains Initiative, which is grateful for the support of CGIAR Trust Fund contributors:[www.cgiar.org/funders](http://www.cgiar.org/funders).

### **Annexure Supplementary Data**

Annexures A and B can be found in the supplementary document.

### **Appendix A. Supporting information**

Supplementary data associated with this article can be found in the online version at [doi:10.1016/j.ejrh.2023.101330](https://doi.org/10.1016/j.ejrh.2023.101330).

### **References**

- Agarwal, S., Patil, J., Goyal, V., Singh, A., 2018. Assessment of Water Supply-Demand Using Water Evaluation and Planning (WEAP) model for Ur River Watershed, Madhya Pradesh, India. *J. Inst. Eng. Ser. A* 100 (1), 21–32.
- Arranz, R. and McCartney, M. 2007. Application of the Water Evaluation and Planning (WEAP) model to assess future water demands and resources in the Olifants Catchment, South Africa. *International Water Management Institute* 116 1–45.
- Ayele, A. 2016. Application of Water Evaluation and Allocation Planning (WEAP) model to assess future water demands and water balance of the Caledon River Basin. Unpublished Doctoral thesis, Department of Civil Engineering, Central University of Technology, Free State, South Africa, Free State, South Africa.
- DARD. 2015. Strategy for agrarian transformation in KwaZulu-Natal. Department of Agriculture and Rural Development (DARD), Pietermaritzburg, South Africa.

- DEA. 2013b. Climate Trends and Scenarios for South Africa. Report No.: 1 of 6. Long-term Adaptation Scenarios Flagship Research Programme (LTAS). Department of Environmental Affairs, Pretoria, South Africa.
- DEA. 2013a. Climate change implications for the water sector in South Africa. Report No.: 2 of 6. Long-Term Adaptation Scenarios Flagship Research Programme (LTAS). Department of Environmental Affairs, Pretoria, South Africa.
- DEA 2012. 2nd South Africa Environmental Outlook, Chapter 8: Inland Water. Department of Environmental Affairs, Pretoria, South Africa.
- Dlamini, D. and Schulze, R. 2006. Assessment of the water poverty index at Meso-Catchment Scale in the Thukela Basin. Unpublished Dissertation thesis, School of Bioresources Engineering and Environmental Hydrology, University of KwaZulu-Natal, Pietermaritzburg, South Africa.
- Dlamini, N. and Mostert, R. 2019. Closure Plan in Support of the Environmental Authorisation for the Proposed Prospecting Right Application for Coal, Pseudocoal, Anthracite, Sand and Clay on the Remainder of the Farm 15454, Remainder of the Farm Highvake 9311, Remainder and Portion 1 of the Farm Lowvale 15596, Remainder of the Farm Ormiston 8195, Remainder and Portion 3 of the Farm Langklip 10711 and Remainder of the Farm 16763, Under Dannhauser Local Municipality, Kwa-Zulu Natal Province. Project Reference: KZN 30/5/1/1/2/10826PR. Thiiko Resources, KwaZulu-Natal, South Africa.
- Droogers, P., Kruijsheer, M., Boer, Fd, Terink, W., Andriessen, M. and Pelgrum, H. 2017. Water balance and allocation modelling in Rwanda. FutureWater, The Netherlands.
- Dube, L., Jury, M., 2003. Structure and precursors of 1992/93 drought in KwaZulu-Natal, South Africa from NCEP reanalysis data. *Water SA* 29 (2), 201–207.
- DWA. 2011. Development of water reconciliation strategy for all towns in the Eastern Region Amajuba District Municipality: First Stage Reconciliation Strategy for Newcastle Water Supply Scheme Area - Newcastle Local Municipality. Contract WP 9712. Department of Water Affairs, Pretoria, South Africa.
- DWAF. 2003. Thukela water management area: overview of water resources availability and utilisation. Report No.: P WMA 07/000/00/0203. Department of Water Affairs and Forestry, Pretoria, South Africa.
- DWS. 2015. uThukela Quaternary Information: Water Management Area 7. Department of Water and Sanitation (DWS): Water Resources of South Africa, Pretoria, South Africa.
- DWS. 2016. Department of Water and Sanitation Spatial Data Download Tool. [Internet]. Available from: <https://gia.dws.gov.za/DWSPortalApplication/>. [Accessed: 10/07/2021].
- DWS. 2018. Hydrology Surface Water. [Internet]. Department of Water and Sanitation. Available from: <https://www.dws.gov.za/Hydrology/Unverified/UnverifiedDataFlowInfo.aspx>. [Accessed: 26/03/2022].
- Erler, A., Frey, S., Khader, O., d'Orgeville, M., Park, Y., Hwang, H., Lapen, D., Peltier, W., Sudicky, E., 2019. Simulating climate change impacts on surface water resources within a lake-affected region using regional climate projections. *Water Resour. Res.* 55 (1), 130–155.
- Exposito, A., Beier, F., Berbel, J., 2020. Hydro-Economic Modelling for Water-Policy Assessment Under Climate Change at a River Basin Scale: A Review. *Water* 12, 1–18.
- Funk, C., Peterson, P., Landsfeld, M., Pedreros, D., Verdin, J., Shukla, S., Husak, G., Rowland, J., Harrison, L., Hoell, A., Michaelson, J., 2015. The climate hazard infrared precipitation with stations - a new environmental record for monitoring extremes. *Sci. Data* 2 (1), 1–21.
- Ghimire, U., Srinivasan, G., Agarwal, A., 2018. Assessment of rainfall bias correction techniques for improved hydrological simulation. *Int. J. Climatol.* 39, 2386–2399.
- Graham, L., Andersson, L., Horan, M., Kunz, R., Lumsden, T., Schulze, R., Warburton, M., Wilk, J., Yang, W., 2011. Using multiple climate change projections for assessing hydrological response to climate change in the Thukela River Basin, South Africa. *Phys. Chem. Earth* 36 (14–15), 727–735.
- Gudmundsson, L., Bremnes, J., Haugen, J., Engen-Skaugen, T., 2012. Downscaling RCM precipitation to the station scale using statistical transformations – a comparison of methods. *Hydrol. Earth Syst. Sci.* 16, 3383–3390.
- Gyamfi, C., Ndambuka, M., Salim, R., 2016. Hydrological responses to land use/cover changes in the Olifants Basin, South Africa. *Water* 8 (12), 588.
- Hadri, A., Saidi, M., Elkhalki, E., Aachrine, B., Saouabe, T., 2022. Integrated water management under climate change through the application of weap model in a Mediterranean Arid Region. *J. Water Clim. Change* 13 (6), 2414.
- Haji, H. 2011. Impact of Climate Change on Surface Water Availability in the Upper Vaal River Basin. Unpublished MSc Thesis thesis, Department of Civil Engineering, Tshwane University of Technology, Pretoria, South Africa.
- Howells, M., Hermann, S., Welsch, M., Bazilian, M., Segerström, R., Alfstad, T., Gielen, D., Rogner, H., Fischer, G., Velthuisen, H., Wiberg, D., Young, C., Roehrl, R., Mueller, A., Steduto, P., Ramma, I., 2013. Integrated analysis of climate change, land-use, energy and water strategies. *Nat. Clim.* 3, 621–626.
- INR. 2019. Environmental Management Framework for the Amajuba District Municipality. Summary Report. Institute of Natural Resources, Pietermaritzburg, South Africa.
- Jiang, L., Wu, H., Tao, J., Kimball, J., Alfrieri, L., Chen, X., 2020. Satellite-based evapotranspiration in hydrological model calibration. *Remote Sens.* 12 (428).
- Kim, T., 2017. Understanding one-way ANOVA using conceptual figures. *Korean J.f Anesthesiol.* 70 (1), 22–26.
- Kruskal, W., Wallis, W., 1952. Use of ranks in one-criterion variance analysis. *J. Am. Stat. Assoc.* 47 (260), 583–621.
- Levite, H., Sally, H., Cour, J., 2003. Testing water demand management scenarios in a water-stressed basin in South Africa: application of the WEAP model. *Phys. Chem. Earth* 28, 779–786.
- LGCCP. 2018. Amajuba district municipality: climate change vulnerability assessment and response plan. Version 2. Local Government Climate Change Support Program (LGCCP), Deutsche Gesellschaft für Internationale Zusammenarbeit (GIZ), Pretoria, South Africa.
- Liu, H. 2015. Comparing Welch ANOVA, a Kruskal-Wallis Test, and Traditional ANOVA in Case of Heterogeneity of Variance. Unpublished MSc thesis, Department of Biostatistics, Virginia Commonwealth University, Richmond, Virginia.
- Mabhaudhi, T., Simpson, G., Badenhorst, J., Mohammed, M., Motongera, T., Senzanje, A. and Jewitt, G. 2018. Assessing the State of the Water-Energy-Food (WEF) Nexus in South Africa. Report No.: KV 365/18. Water Research Commission, Pretoria, South Africa.
- Mausser, W., Klepper, G., Zabel, F., Delzeit, R., Hank, T., Putzenlechner, B., Calzadilla, A., 2015. Global biomass production potentials exceed expected future demands without the need for cropland expansion. *Nat. Commun.* 6 (1), 1–11.
- McNamara, I., Nauditt, A., Penedo, S. and Ribbe, L. 2018. NEXUS Water-Energy-Food Dialogues Training Material: Introduction to the Water-Energy-Food Security (WEF) NEXUS. Training Unit 01. The Nexus Dialogue Programme, Bonn and Eschborn, Germany.
- Moriasi, D., Arnold, J., vanLiew, M., Bingner, R., Harmel, R., Veith, T., 2007. Model evaluation guidelines for systematic quantification of accuracy in watershed integration. *Am. Soc. Agric. Biol. Eng.* 50 (3), 885–900.
- Ndlovu, M., Demlie, M., 2020. Assessment of meteorological drought and wet conditions using two drought indices across KwaZulu-Natal Province, South Africa. *Atmosphere* 11 (6), 623(1-20).
- Parra, V., Fuentes-Aguilera, P., Munoz, E., 2018. Identifying advantages and drawbacks of two hydrological models based on a sensitivity analysis: a study in two Chilean watersheds. *Hydrol. Sci. J.* 63 (12), 1831–1843.
- Savva, A.P. and Frenken, K. 2002. Module 4: Crop Water Requirements and Irrigation Scheduling. In: FAO Irrigation Manual, Water Resources Development and Management Officers, FAO Sub-Regional Office for East and Southern Africa.
- Schütte, S., Schulze, R.E. and Clark, D.J. 2022. A national assessment of potential climate change impacts on the hydrological yield of different hydro-climatic zones of South Africa. WRC Report No. K5/2833/1&2. Water Research Commission, Pretoria, South Africa.
- Shabalala, I. and Mthembu, S. 2022. Nquthu Local Municipality 2022/23–2026/27 Integrated Development Plan. KwaZulu-Natal, South Africa.
- Sieber, J. 2015. Water Evaluation And Planning (WEAP) User Guide. Stockholm Environment Institute, Somerville, United States of America.
- StatsSA. 2010. Water management areas in South Africa. Discussion documeny: DO405.8. Statistics South Africa.
- StatsSA. 2017. Census of commercial agriculture 2017 - KwaZulu-Natal. Report No.: 11–02-06. Statistics South Africa, Pretoria, South Africa.
- Tena, T., Mwaanga, P., Nguvulu, A., 2019. Hydrological modelling and water resources assessment of chongwe river catchment using WEAP Model. *Water* 11 839 (1–17).
- Thompson, A., Calvin, K., Smith, S., Kyle, G., Volke, A., Patel, P., Delgado-Arias, S., Bond-Lamberty, B., Wise, M., Clarke, L., Edmonds, J., 2011. RCP 4.5: a pathway for stabilization of radiative forcing by 2100. *Clim. Change* 109 (1), 77–94.

- Thrasher, B., Maurer, E., McKellar, C., Duffy, P., 2012. Technical note: bias correcting climate model simulated daily temperature extremes with quantile mapping. *Hydrol. Earth Syst. Sci.* 16, 3309–3314.
- Tramblay, Y., Jarlan, L., Hanich, L., Somot, S., 2018. Future scenario of surface water resources availability in North African dDams. *Water Resour. Manag.* 32 (4), 1291–1306.
- uMgeni. 2016. Universal Access Plan Phase 2 - Progressive Development of a Regional Concept Plan for the Amajuba District Municipality Newcastle Local Municipality. UAP Phase 2 Report. uMgeni Water Pretoria, South Africa.
- uMgeni. 2019. Universal Access Plan Phase iii: Progressive Development of a Regional Concept Secondary Bulk Water Master Plan for the Amajuba District Municipality (WSA) and Newcastle Local Municipality. uMgeni Water, Pietermaritzburg, South Africa.
- uMgeni. 2020. Infrastructure Master Plan 2020 (2020/2021–2050/2051): Buffalo System. UMgeni Water, Pietermaritzburg, South Africa.
- uMgeni. 2021. Universal Access Plan Phase III - Progressive Development of a Regional Concept Secondary Bulk Water Master Plan for the Umzinyathi District Municipality. Umgeni Water, Pietermaritzburg, South Africa.
- Vuuren, D.V., Edmonds, J., Kainuma, M., Riahi, K., Thompson, A., Hibbard, K., Hurtt, G., Kram, T., Krey, V., Lamarque, J., Masui, T., 2011. The representative concentration pathways: an overview. *Clim. Change* 109 (1), 5–31.
- Wayne, G. 2013. The Beginner's Guide to Representative Concentration Pathways, Version 1.0. [Internet]. Skeptical Science. Available from: [www.skepticalscience.com](http://www.skepticalscience.com). [Accessed: 30/07/2021].
- Welsch, M., Hermann, S., Howells, M., Rogner, H., Young, C., Ramma, I., Bazilian, M., Fischer, G., Alfstad, T., Gielen, D., Blanc, D., Rohrl, A., Steduto, P., Muller, A., 2014. Adding value with CLEWS – modelling the energy system and its interdependencies for Mauritius. *Appl. Energy* 113, 1434–1445.
- WMO 2021. Updated 30-year Reference Period Reflects Changing Climate. [Internet]. World Meteorological Organization. Available from: <https://public.wmo.int/en/media/news/updated-30-year-reference-period-reflects-changing-climate>. [Accessed: 24/08/2022].